Available online at www.sciencedirect.com
ScienceDirect
Neural Networks 19 (2006) 1329–1346
Neural Networks
www.elsevier.com/locate/neunet

2006 Special Issue

Selective attention through phase relationship of excitatory and inhibitory input synchrony in a model cortical neuron

Jyoti Mishra[a,*], Jean-Marc Fellous[b,1], Terrence J. Sejnowski[a,c]

[a] *Division of Biological Sciences, University of California, San Diego, La Jolla, CA 92093, United States*
[b] *Department of Biomedical Engineering and Center for Cognitive Neuroscience, Duke University, Durham, NC 27708, United States*
[c] *Howard Hughes Medical Institute, Computational Neurobiology Laboratory, Salk Institute, La Jolla, CA 92037, United States*

Received 30 June 2006; accepted 1 August 2006

Abstract

Neurons in area $V2$ and $V4$ exhibit stimulus specific tuning to single stimuli, and respond at intermediate firing rates when presented with two differentially preferred stimuli ('pair response'). Selective attention to one of the two stimuli causes the neuron's firing rate to shift from the intermediate pair response towards the response to the attended stimulus as if it were presented alone. Attention to single stimuli reduces the response threshold of the neuron and increases spike synchronization at gamma frequencies. The intrinsic and network mechanisms underlying these phenomena were investigated in a multi-compartmental biophysical model of a reconstructed cat $V4$ neuron. Differential stimulus preference was generated through a greater ratio of excitatory to inhibitory synapses projecting from one of two input $V2$ populations. Feedforward inhibition and synaptic depression dynamics were critical to generating the intermediate pair response. Neuronal gain effects were simulated using gamma frequency range correlations in the feedforward excitatory and inhibitory inputs to the $V4$ neuron. For single preferred stimulus presentations, correlations within the inhibitory population out of phase with correlations within the excitatory input significantly reduced the response threshold of the $V4$ neuron. The pair response to simultaneously active preferred and non-preferred $V2$ populations could also undergo an increase or decrease in gain via the same mechanism, where correlations in feedforward inhibition are out of phase with gamma band correlations within the excitatory input corresponding to the attended stimulus. The results of this model predict that top-down attention may bias the $V4$ neuron's response using an inhibitory correlation phase shift mechanism.

Keywords: Selective attention; $V4$; Gain modulation; Gamma band synchrony; Out of phase inhibition

1. Introduction

Neural correlates of selective attention have been studied using single-unit recordings from primate extrastriate area $V4$. It was found that attention increases the neuron's firing rate in response to a single stimulus placed in its receptive field. When more than one stimulus is presented, selective attention can modulate the neuron's response based on its stimulus selectivity. When attention is directed to the neuron's preferred stimulus the neuron's firing rate is increased; when attention is directed to the non-preferred stimulus its firing rate is decreased (Reynolds, Chelazzi, & Desimone, 1999; Reynolds, Pasternak, & Desimone, 2000; Reynolds & Desimone, 2003). This phenomenon has been conceptually explained as a biased competition (Desimone & Duncan, 1995; Reynolds et al., 1999) wherein active $V2$ input populations from multiple stimuli compete with one another to generate a $V4$ neuronal response intermediate between the responses to the individual stimuli. Attending to a stimulus can bias this competition producing a shift in the $V4$ neuron's response towards the response that would be obtained if the attended stimulus population was active alone.

Several models have been proposed to elucidate the mechanisms underlying stimulus competition and attentional bias. In a phenomenological model by Reynolds et al. (1999), attention bias was conceived as an increase in the synaptic

* Corresponding address: Division of Biological Sciences, University of California, San Diego, 9500 Gilman Drive MC 0608, La Jolla, CA 92093-0608, United States. Tel.: +1 858 534 5562; fax: +1 858 534 1566.
E-mail address: jmishra@ucsd.edu (J. Mishra).
[1] Present address: University of Arizona, Neural Systems Memory and Aging, Life Sciences North, #384, Tucson, AZ, 85724, United States.

0893-6080/$ - see front matter © 2006 Elsevier Ltd. All rights reserved.
doi:10.1016/j.neunet.2006.08.005

weights of the inputs from the neurons that receive visual information from the attended stimulus. However, the time course of synaptic modification being generally slow, it is not clear how such synaptic biases can emerge at the time scales of attention shifts. In other network models cell populations selective to specific stimulus features such as orientation were used with feedforward and feedback connections to a global inhibitory network pool. In the presence of multiple stimuli, a principal cell's response to a preferred stimulus was suppressed by inhibitory inputs recruited from other principal cells that selectively responded to the non-preferred stimuli (Deco, Pollatos, & Zihl, 2002; Usher & Niebur, 1996). The competition was biased in favor of a particular feature/ orientation by providing an external excitatory top-down drive preferentially to the principal cells tuned to that orientation. Hence, the attention effect was modeled by modulating the total amount of input excitation and inhibition to a neuron. In a single cell multicompartmental model, stimulus competition was implemented by spatially segregating the inputs projecting onto a $V4$ neuron to different regions of its dendritic tree (Archie & Mel, 2000). The authors also modeled the attentional bias by increasing the amount of feedforward excitatory input to the attended stimulus (Archie & Mel, 2004).

The above models hypothesize that a neuron must receive increased excitatory inputs to exhibit attentional modulation. This increase assumes the existence of a mechanism that can recruit new excitatory inputs, or that can selectively increase the firing rate of the input population corresponding to the attended stimulus. An alternative hypothesis is that the amount of excitatory inputs (number or rate) remains unchanged, but that attentional bias is achieved by a modulation of their correlation. Correlations imply no change in the sum total input spikes to a neuron, nor a change in synaptic strengths, but a possibly rapid change in the relative spike timing of these inputs such that spikes from different neurons arrive close together in time and have therefore a greater postsynaptic impact.

Model simulations have shown that input correlations increase the gain of a post-synaptic neuron's input–output firing rate curve (Chance, Abbott, & Reyes, 2002; Fellous, Rudolph, Destexhe, & Sejnowski, 2003; Salinas & Sejnowski, 2000, 2002). This is achieved by increased fluctuations around the spiking threshold of the neuron. Correlation in either the excitatory or inhibitory inputs can separately elicit this effect; however correlations between excitatory and inhibitory input annul this increase in gain. Physiologically, correlations have been observed as gamma frequency range oscillations in visual cortex (reviewed in Engel, Roelfsema, Fries, Brecht, and Singer (1997), Singer (1999), Singer and Gray (1995)), and neuronal assemblies that have a common orientation preference to synchronize with one another (Eckhorn et al., 1988; Gray & Singer, 1989; Gray, Engel, Konig, & Singer, 1990). More recently $V4$ neurons receiving their preferred stimulus input have been shown to have spike field coherence in the gamma frequency range in spatial attention (Fries, Reynolds, Rorie, & Desimone, 2001) as well as visual search tasks (Bichot, Rossi, & Desimone, 2005). In addition to excitatory neurons, there is vast accumulating evidence that networks of inhibitory interneurons mutually synchronize and are capable of generating gamma frequency range oscillations in the hippocampus and cortex (Deans, Gibson, Sellitto, Connors, & Paul, 2001; Fisahn, Pike, Buhl, & Paulsen, 1998; Wang & Buzsaki, 1996). Based on model simulations it was proposed that the attention effects to single stimuli could be mediated by the modulation of the synchrony of interneuron networks (Tiesinga, Fellous, Salinas, Jose, & Sejnowski, 2004). In this model when the temporal dispersion of the inhibitory inputs to the $V4$ neuron was reduced, leading to greater synchrony, the neuron displayed a firing rate gain akin to that seen when a stimulus is attended. However, increasing the synchrony of the interneuron network corresponding to an attended stimulus always increased the model response. Hence a synchrony manipulation on its own cannot account for a decrease in firing when a non-preferred stimulus is attended.

Recently Tiesinga (2005) also proposed an inhibitory correlation mechanism for biased stimulus competition termed stimulus competition by inhibitory interference. The firing rate of the postsynaptic neuron was modulated with attention to the preferred or non-preferred stimulus by changing the phase delay between two separate inhibitory populations that represented either stimulus. When the two inhibitory populations oscillating in the gamma frequency range were in phase or had constructive interference the postsynaptic neuron's firing rate was increased. A reduction in firing rate was achieved when the two inhibitory populations were out of phase. In this model excitatory inputs were modeled as asynchronous events, which may not be entirely compatible with evidence from recordings in striate and extrastriate cortex (reviewed in Engel et al. (1997), Singer (1999), Singer and Gray (1995)). Given the evidence for synchronized oscillation in both excitation and inhibition in cortex we investigate a mechanism wherein both these components are correlated to attain biased stimulus competition.

2. Methods

2.1. Model and quantitative assumptions

We used a multi-compartmental reconstruction of a layer 4 spiny stellate neuron (Mainen & Sejnowski, 1996) to represent the $V4$ neuron in our model. Voltage gated Na^+ and K^+ Hodgkin–Huxley channels were inserted in the soma and axon. The soma was also provided with a M-type K^+ current to allow for spike frequency adaptation as well as Ca^{2+} dependent K^+ after-hyperpolarizing currents that prevented excessive spike bursts to synaptic inputs. The dendrites were modeled as passive and all compartments were provided with a gradient of leak currents as determined experimentally (Stuart & Spruston, 1998).

The $V4$ neuron received stimulus driven feedforward excitatory and inhibitory synaptic input from cortical area $V2$ as well as stimulus independent synaptic inputs that represented intracortical or top-down inputs (Fig. 1). All glutamatergic inputs were distributed uniformly throughout the dendritic tree, while inhibitory inputs were located perisomatically within

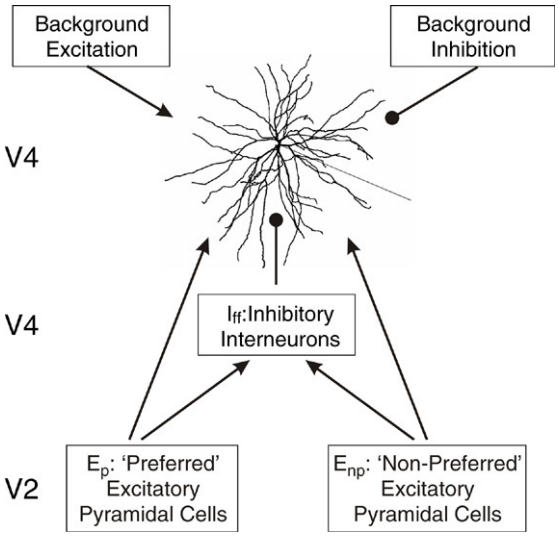

Fig. 1. Schematic representation of the excitatory and inhibitory synaptic inputs projecting onto the multicompartmental $V4$ neuron model. Two excitatory synaptic input pools were provided to represent the two competing stimuli projecting from $V2$. The 'Preferred' excitatory input (E_p) had a greater number of glutamatergic synapses (400 in most simulations) than the 'Non-Preferred' (E_{np}, 100 synapses). A single feedforward inhibitory interneuron pool (I_{ff}) was used with 80 GABAergic synapses. The firing rate of the inhibitory synaptic inputs was a linear function of the firing rate of the active $V2$ excitatory pool (s) (see Section 2). The $V4$ neuron also received continuous uncorrelated background excitatory and inhibitory synaptic inputs, containing 5000 and 920 synapses respectively. Arrows represent excitatory projections, filled circles represent inhibitory projections.

200 μm of the soma. Glutamatergic $V2$ inputs were provided from two separate synaptic populations with a number of synapses ranging from 100 to 400 synapses. This number of $V2$ projections was approximated from anatomical observations (Ahmed, Anderson, Douglas, Martin, & Nelson, 1994). It is known that neurons in area $V2$ and $V4$ are tuned to visual features such as orientation and color. The two input $V2$ synaptic populations represented the preferred (E_p) and non-preferred (E_{np}) stimulus driven inputs. The number of excitatory synapses projecting from the preferred population was set at 400 while non-preferred input was modeled with 100 synapses (Fig. 1) for all simulations investigating the effects of paired visual stimuli on the $V4$ neuron.

The number of inhibitory synapses was chosen as per anatomical data that suggested that synaptic inputs to a layer 4 visual cortical neuron consisted of approximately 80% excitatory synapses and 20% inhibitory synapses (Anderson, Douglas, Martin, & Nelson, 1994; Beaulieu, Kisvarday, Somogyi, Cynader, & Cowey, 1992; Fitzpatrick, Lund, Schmechel, & Towles, 1987). In our simulations, feedforward inhibition (I_{ff}) was provided by a pool of 80 GABAergic synapses (Fig. 1). The firing rate F_i of the feedforward inhibitory synapses was modeled as a linear function of the firing rate of the total active excitatory $V2$ input.

$$F_i = \alpha(F_p + F_{np}). \tag{1}$$

When only one of the two excitatory $V2$ input populations was active, there was no dependence of F_i on the inactive $V2$ population. Inhibition was thus modeled as broadly tuned as has been reported in studies in ferrets and primates (Ringach, Hawken, & Shapley, 1997; Roerig & Chen, 2002). Recent intracellular recordings in cat striate cortex have also revealed that excitatory and inhibitory inputs are often iso-orientation tuned but may also be tuned to different orientations in a large fraction of neurons, thus exhibiting broad tuning at the population level (Monier, Chavane, Baudot, Graham, & Fregnac, 2003). The value of α in our model was set to 3 because fast-spiking inhibitory neurons are known to spike at much higher firing rates than excitatory neurons (Lacaille & Williams, 1990; McCormick, Connors, Lighthall, & Prince, 1985) and because electrophysiological recordings in primary visual cortex reported inhibition to be 2–3 fold stronger than excitation (Anderson, Carandini, & Ferster, 2000).

The numbers of top-down synaptic connections to the $V4$ neuron were set at 5000 independent background excitatory and 920 background inhibitory synapses (Fig. 1). Presynaptic firing rates at these synapses were held constant when simulating the effects of visual stimulation to the $V4$ neuron. In order to maintain a spontaneous firing rate of 2–5 Hz in the $V4$ neuron under no input conditions (Luck, Chelazzi, Hillyard, & Desimone, 1997), the maintained firing rate of the top-down excitatory inputs to the synapses was set according to a Poisson distribution at 1.5 Hz, the top-down inhibitory inputs at 7.5 Hz, and the $V2$ excitatory/ inhibitory input at 3 Hz respectively.

2.2. Dynamic stochastic synaptic input

Excitatory synaptic inputs to the $V4$ neuron were modeled with probabilistic release kinetics yielding short-term facilitation and depression (Fellous, Buntaine, Hoang, & Bhanpuri, 2006; Maass & Zador, 1999; Stevens & Wang, 1995; Wang, Fellous, Spencer, & Sejnowski, in preparation). Inhibitory inputs were deterministic. The postsynaptic current was described by an alpha function so that

$$I_{\text{syn}} = G_{\max} \times G \times (V - E_{\text{rev}}) \tag{2}$$

$$G(t) = G(t) + s \times (t - t_0) \times \mathrm{e}^{-\frac{(t-t_0)}{\tau}} \tag{3}$$

where t_0 is the last time of successful release and $s = 50$ μS.

For excitatory synapses $G_m = 1$ nS; $E_r = 0$ mV; $\tau = 3$ ms and for inhibitory synapses $G_m = 0.1$ nS; $E_r = -80$ mV; $\tau = 5$ ms. Only AMPA and GABA_A postsynaptic effects were modeled here. NMDA effects were not modeled explicitly as they are temporally much slower than the time scales considered here (around gamma frequencies).

For excitatory synapses the probability of release at time t at each synapse, P_r followed

$$P_r(t) = 1 - \mathrm{e}^{-F(t)D(t)} \tag{4}$$

where $F(t)$ and $D(t)$ represented facilitation and depression dynamics respectively, and were given by

$$F(t) = F_0 + F_m.\mathrm{e}^{-(t-t_o)/\tau_F} \tag{5}$$

$$D(t) = D_0 - D_m.\mathrm{e}^{-(t-t_r)/\tau_D} \tag{6}$$

where $F_0 = 0.003$; $F_m = 0.02$; $\tau_F = 94$ ms; $D_0 = 40$; $D_m = 15$; $\tau_D = 380$ ms; t_o is the time of the last

presynaptic spike arriving at the synapse obtained from an independent Poisson distribution, and t_r is the last time at which a successful neurotransmitter release has occurred. Note that because of the stochastic nature of the synapse, t_o and t_r are not necessarily identical. These values were tuned to match experimental data in vitro (Dobrunz & Stevens, 1997, 1999; Fellous et al., 2006) and are in good agreement with other phenomenological models in cortex (Varela et al., 1997) (not shown).

2.3. Correlated synaptic inputs

In order to simulate correlated excitatory or inhibitory synaptic input in the gamma frequency range from a set of N synapses, M Poisson distributed presynaptic spike times at each of the N synapses were created with a periodic distribution of $T = 25$ ms (i.e. 40 Hz). The firing rate at each synapse remained constant. In our simulations, N contained either 30%, 50% or 80% of the total synapses from a particular population. Not more than $M = 25$ of the total presynaptic times (chosen randomly) at every excitatory synapse were periodically distributed as it is known that not all spikes from a given cell may participate in a particular synchronously oscillating assembly (Buzsaki & Chrobak, 1995; Singer, 1999). The value of M was pre-calculated to generate maximum correlation to the gamma rhythm at 40 Hz firing frequency. The periodic distribution of spike times was provided with a jitter of 3 ms, unless stated otherwise.

All simulations were performed with version 5.7 of the NEURON program using a 0.1 ms time step and simulated temperature of 36 °C (Hines & Carnevale, 2001). Simulation results were obtained on the basis of 20 trials. In all trials, the $V4$ neuron was simulated for 300 ms (pre-stimulus baseline) in conditions of background synaptic inputs as specified above. At 300 ms the $V4$ neuron was stimulated by providing a higher than baseline firing rate input from one (or both) set(s) of $V2$ excitatory (and the appropriate accompanying inhibitory) synapses. In all simulations, stimuli remained active for 350 ms in order to replicate the stimulation period in attention experiments where firing rate modulation of $V4$ neurons is observed (Luck et al., 1997; Reynolds et al., 1999).

Fig. 2 shows the stimulus response of the $V4$ neuron over time in single as well as multiple trials. The $V2E_p$ or 'preferred' input population was activated at 40 Hz firing rate in this case. The neuron responded with a large number of initial spikes to the stimulus and its firing rate settled to a lower value beyond the first 100 ms of stimulation. Such an adapting response of the neuron emerged from its intrinsic channel properties as well as from input synaptic dynamics, as will be discussed below.

3. Results

3.1. Stimulus preference: Tuning by synapse number

Neurons in area $V4$ display tuning to features of visual stimuli such as orientation and color as well as their combinations. We first generated the neuronal connectivity from $V2$ to $V4$ that gave rise to such stimulus tuning. For this purpose the $V2$ population encoding the preferred stimulus feature projected to the $V4$ neuron with the maximum number of excitatory synapses used in our simulations (400). This population shown in Fig. 1 is the preferred E_pV2 population.

$V2$ populations representing less preferred stimuli projected to $V4$ with a smaller number of excitatory synapses. As stated in the methods, the number of synapses in the feedforward inhibitory pool I_{ff} was kept constant at 80 synapses, but the firing rate of the GABAergic neurons was modulated linearly as a function of the active $V2$ populations. Hence, we assume that each stimulus feature activates a specific set of excitatory $V2$ neurons, but the same set of feedforward $V4$ inhibitory neurons. Consequently, the ratio of excitatory to inhibitory synapses is greater for the preferred $V2$ population and smaller for a non-preferred $V2$ population. This assumption is essentially similar to the simple biased competition model of Reynolds et al. (1999) except that the preferred and non-preferred stimuli are not provided with distinct inhibitory pools.

The response of the $V4$ neuron to a 40 Hz firing rate input from the preferred $V2$ population consisting of 400 synapses is depicted in Fig. 2. We simulated the neuron's response to a range of input firing rates from 0 to 80 Hz. The average firing rate was calculated for the 350 ms stimulation period. Fig. 3(A) shows the average firing rate response curve for the $V4$ neuron to increasing firing rate from a $V2$ population with either 400, 300 or 100 synapses. The $V2$ population that projects 100 excitatory synapses generated a near baseline firing rate of 1–6 Hz in the $V4$ neuron. This represented the 'non-preferred' stimulus population in our model. The $V4$ neuron exhibited baseline firing rates of 1–3 Hz when the $V2$ synapse population was inactive (0 Hz) because feedforward and top-down inputs to the neuron yielded some spontaneous firing in the absence of stimuli (see Section 2).

The $V4$ neuron's response to increasing input saturated at high firing rates principally because of presynaptic depression of excitatory synaptic inputs (see Section 2). Increasing feedforward inhibitory input at high firing rates did contribute to response saturation, but saturation persisted in the model even in the absence of such inhibition (not shown). The intrinsic I_M and K_{AHP} currents in the soma did not specifically contribute to spike saturation at high firing rates. Excluding these channels negligibly shifted the entire firing rate curve upwards (not shown). Firing rate saturation was always seen at $V2$ input rates beyond 40–50 Hz independent of stimulus preference. This saturation effect was similar to the modeled effects of thalamacortical synaptic depression on $V1$ neurons for high contrast stimuli (Carandini, Heeger, & Senn, 2002). The overall firing rate range observed in our model was similar to the firing rate responses of $V4$ neurons seen physiologically (Luck et al., 1997; McAdams & Maunsell, 1999; Reynolds et al., 1999). We noted though that spikes at the highest input firing rates of 70–80 Hz show slight response suppression post-saturation. This is perhaps because we simplistically modeled inhibition without synaptic depression. Hence, while excitation depressed at high firing rates, inhibition stayed strong in the model. Inhibitory synaptic depression has been reported in

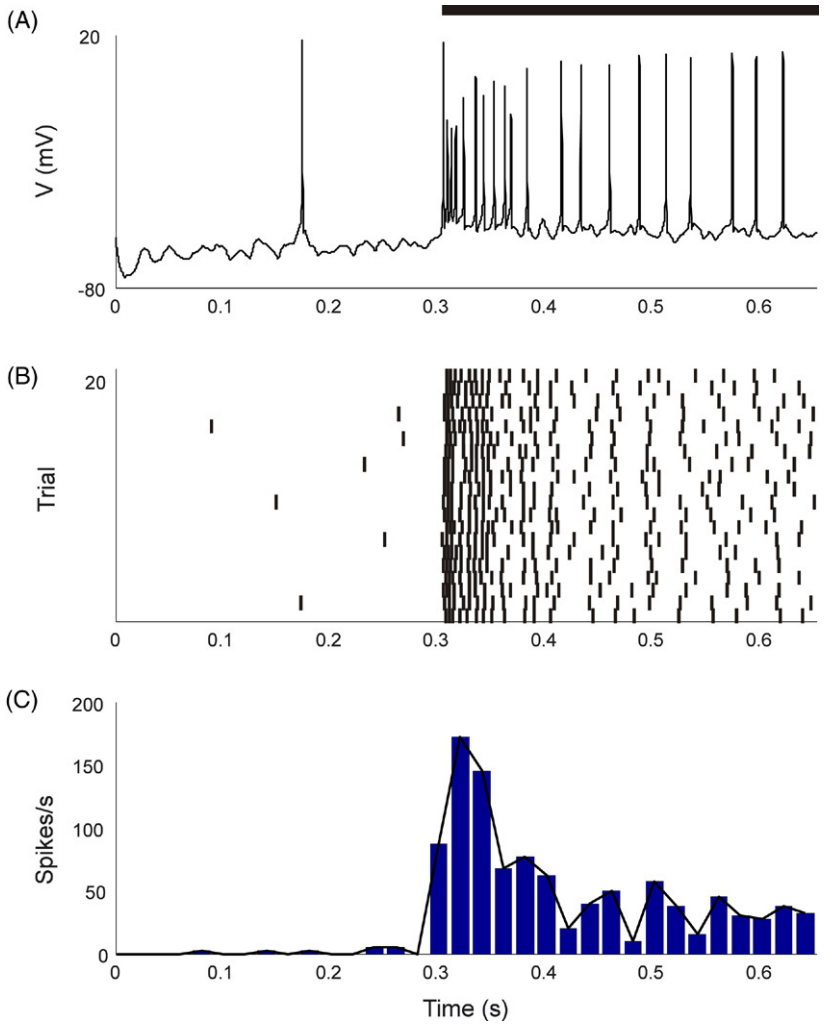

Fig. 2. Response of the modeled $V4$ neuron to the preferred stimulus. The black bar represents the stimulation period from 300 to 650 ms where the firing rate of the 400 $V2$ excitatory (E_p) synapses was stepped from a baseline firing rate of 3 Hz to a firing rate of 40 Hz. The firing rates of the 80 inhibitory (I_{ff}) synapses were also increased accordingly. (A) Single trial spike response of neuron. (B) Rastergram of per trial spike responses for 20 trial runs. (C) Average firing rate spike histogram of the neuronal spike train. The overlaid black line is a continuous plot representation of the same histogram. Data from the 20 trial runs were averaged in 20 ms time bins.

visual cortex (Varela, Sen, Turrigiano, & Nelson, 1999) but it is much smaller than excitatory depression. Also because of a lack of adequate quantitative data in $V4$, we chose not to model this type of depression at this time.

Stimulus tuning can be successfully generated with the synapses distributed randomly and uniformly on the entire dendritic tree of the $V4$ neuron. Moreover, stimulus tuning is negligibly altered if the synapses are provided with a different random distribution placement (not shown). This formulation is different from that of Archie and Mel (2000) where the authors generate tuning by distinct spatial arrangement of synapses representing the preferred and non-preferred $V2$ populations. Fig. 3(B) shows the stimulus tuning curve for the modeled $V4$ neuron at increasing input firing rates from 5 to 50 Hz, assuming that stimulus preference (such as orientation) was due to the recruitment of a proportional number of presynaptic $V2$ neurons. The multiplicative stimulus tuning achieved was similar to experimental data on orientation tuning obtained in macaque and cat striate cortex (Albrecht & Hamilton, 1982; Albrecht, Geisler, Frazor, & Crane, 2002; Carandini, Heeger, & Movshon, 1997; Sclar & Freeman, 1982) and macaque $V4$ (McAdams & Maunsell, 1999) for stimuli with increasing contrast.

3.2. Responses of the $V4$ neuron to stimulus pairs

It has been shown that when two differentially preferred visual stimuli are simultaneously presented in a $V4$ neuron's receptive field, the neuron responds with a firing rate in between the firing rates obtained when either stimulus is presented alone (Reynolds et al., 1999). With the synaptic connectivity in our model as described above we were able to generate such a response to paired stimuli. For this purpose, the number of synapses projecting from the non-preferred $V2$ population or E_{np} was set at 100. We simulated the response to stimulus pairs for three preferred $V2$ populations E_p that respectively had 400 (Fig. 4(A)), 300 (Fig. 4(B)) and 100 (Fig. 4(C)) synapses. The firing rate of both $V2$ populations was varied from 0 to 80 Hz. The firing rate of the inhibitory pool scaled as described in

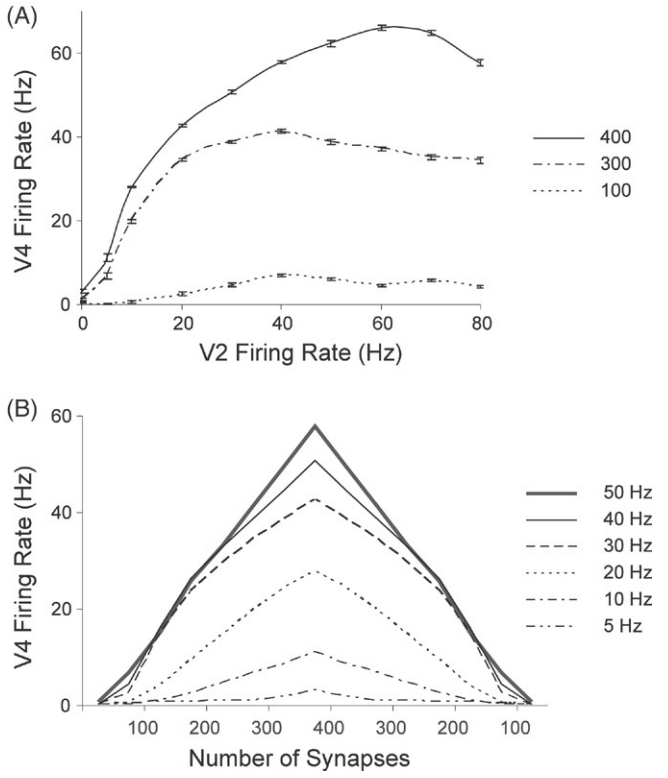

Fig. 3. Stimulus tuning of the modeled $V4$ neuron. (A) An input–output firing rate curve of the $V4$ neuron for different stimulus preferences. Different stimuli are represented in the model by different number of excitatory synapses projecting from $V2$. Simulations were performed with only a single $V2$ excitatory population active. The solid black line represents the preferred stimulus response with 400 synapses. A less preferred stimulus (dot dashed line) was simulated with 300 synapses. The dotted line represents the non-preferred stimulus with 100 synapses. The error bars denote the standard error of the mean response at the different input firing rates (that are analogous to stimulus contrasts). (B) Stimulus tuning in the $V4$ neuron scales multiplicatively. The stimulus parameter on the abscissa is represented in the model by the number of projecting $V2$ excitatory synapses. The neuron's response is maximal for the largest number of $V2$ synapses modeled i.e. 400. The successive plots from bottom to top plot the stimulus tuning at increasing $V2$ input firing rate from 5 to 50 Hz.

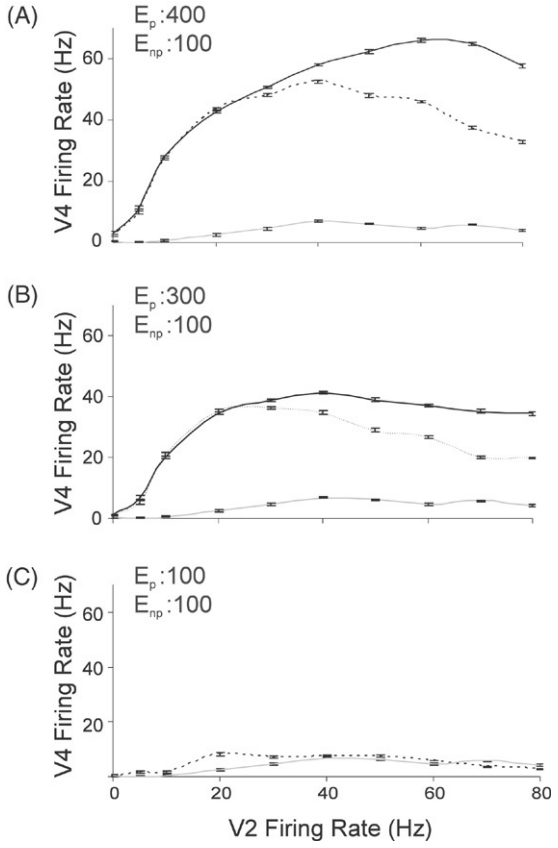

Fig. 4. Response of the modeled $V4$ neuron to pairs of differentially preferred stimuli. The average firing rate response of the $V4$ neuron to increasing firing rate of the $V2$ excitatory input is depicted. Response to the preferred stimulus alone (when only $V2\,E_p$ is active) is in solid black, and to the non-preferred stimulus alone (when only $V2\,E_{np}$ is active) is in light gray. Response to both populations being active at equivalent firing rates is represented by the dashed black line. In all cases E_{np} is modeled with 100 excitatory synapses. In (A), (B) and (C) E_p has 400, 300 and 100 active synapses respectively. As E_p and E_{np} become equally preferred, their responses overlap when activated alone, and hence the solid black line is not visible (C).

Methods. As shown in Fig. 4, at low firing rates of $V2$ input, an intermediate level of $V4$ firing was not observed. Instead the $V4$ neuron's response follows the preferred stimulus. But at higher firing rates of the two input $V2$ populations the firing rate of the $V4$ neuron fell to an intermediate level between firing rates observed for independent activation of the two $V2$ populations. Moreover, if the two $V2$ inputs were equally preferred as was the case in Fig. 4(C) where both populations had 100 projecting synapses, the output neuron showed an additive response at low firing rates.

The increasing firing rates of the two $V2$ populations in our model can be compared to increasing contrasts of presented visual stimuli in physiological experiments (Reynolds & Chelazzi, 2004). These results are also compatible with experiments studying the responses to differentially preferred motion stimuli in macaque area MT (Heuer & Britten, 2002). These experimental data showed that response to pairs tended to follow the response to the more effective stimulus of the pair and was less influenced by the less effective stimulus. Responses to stimulus pairs at varying contrast summed at low contrast while responses fell to intermediate firing rates at high contrasts. Thus our simulations propose a biophysical mechanism explaining these data. At low contrasts, the drive to $V4$ is dominated by the preferred $V2$ population. At sufficiently high firing rates (higher contrasts), those synapses depress and feedforward inhibition I_{ff} takes over and decreases the $V4$ firing rate to intermediate levels.

Reynolds and Desimone (2003) performed an experiment where the response of a $V4$ neuron was measured in the presence of a preferred stimulus when the non-preferred stimulus was presented at successively increasing contrast values. In these experiments the contrast of the preferred stimulus was kept constant. It was found that with increasing non-preferred stimulus contrast the response of the $V4$ neuron was systematically depressed. Earlier reports have also shown that a poor stimulus to a neuron suppresses its response to a preferred stimulus (Miller, Gochin, & Gross, 1993; Recanzone, Wurtz, & Schwarz, 1997; Rolls & Tovee, 1995).

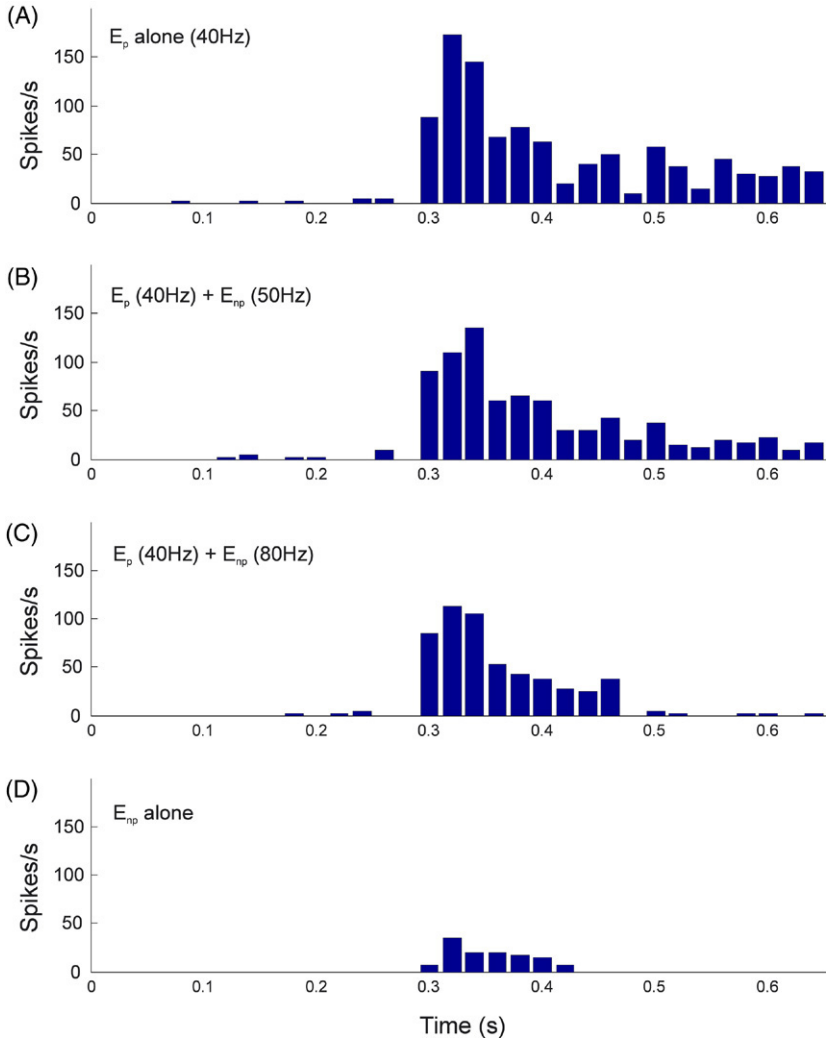

Fig. 5. Time course of the modeled $V4$ neuron response to different firing rate combinations of the preferred and non-preferred synaptic inputs. (A) Spike histogram for the preferred input population E_p (400 synapses) active alone at 40 Hz input firing rate. (B) Spike time histogram with E_p firing at 40 Hz combined with E_{np} or the non-preferred stimulus population (100 synapses) firing at 50 Hz or 80 Hz (C). (D) $V4$ response to E_{np} active alone at 40 Hz firing rate.

There is also substantial evidence for response suppression by presentation of superimposed orientation stimuli orthogonal to the preferred orientation in striate cortex (Bonds, 1989; Carandini et al., 1997; DeAngelis, Robson, Ohzawa, & Freeman, 1992; Morrone, Burr, & Maffei, 1982) as well as in extrastriate cortex (Qian & Andersen, 1994; Snowden, Treue, Erickson, & Andersen, 1991).

We simulated the competition between preferred and non-preferred stimuli and show the results in Fig. 5. The preferred stimulus population E_p was modeled with 400 synapses while the non-preferred population E_{np} had 100 active synapses, as before. Fig. 5(A) depicts the peri-stimulus spike histogram (PSTH) of the $V4$ neuron when only the preferred input E_p synapses were active at 40 Hz firing rate. In Fig. 5(B) and (C), E_{np} was also active along with E_p at 50 Hz and 80 Hz respectively, simulating an increase of contrast of the non-preferred stimulus. The $V4$ neuron's spikes were noticeably depressed with greater firing of E_{np}, especially in the later half of the stimulation period (0.4–0.65 s). Fig. 5(D) shows the PSTH when the non-preferred stimulus was presented alone.

These simulations were performed for the entire firing rate range of the preferred $V2$ population from 0 to 80 Hz combined with different levels of activity of the non-preferred $V2$ population as shown in Fig. 6(A). The solid black curve shows the response of the $V4$ neuron to 0–80 Hz firing of the preferred $V2$ population in the absence of activity of the non-preferred $V2$ input. When the non-preferred $V2$ population was activated at a low firing rate of 20 Hz, the response curve to the preferred stimulus was negligibly affected. However, at higher firing rates of the non-preferred $V2$ population of 50 Hz and 80 Hz, the firing rate of the $V4$ neuron was progressively suppressed at all $V2\,E_p$ firing rate levels. In these simulations, the suppression of firing rate was due to the successively increasing firing rate of the feedforward inhibitory input population I_{ff}.

We also simulated the effect of adding increasing activation of the preferred stimulus to the response curve of the non-preferred stimulus. This is shown in Fig. 6(B) where the preferred $V2$ population spiked at 10 Hz, 40 Hz and 70 Hz together with the non-preferred stimulus. At low firing rates

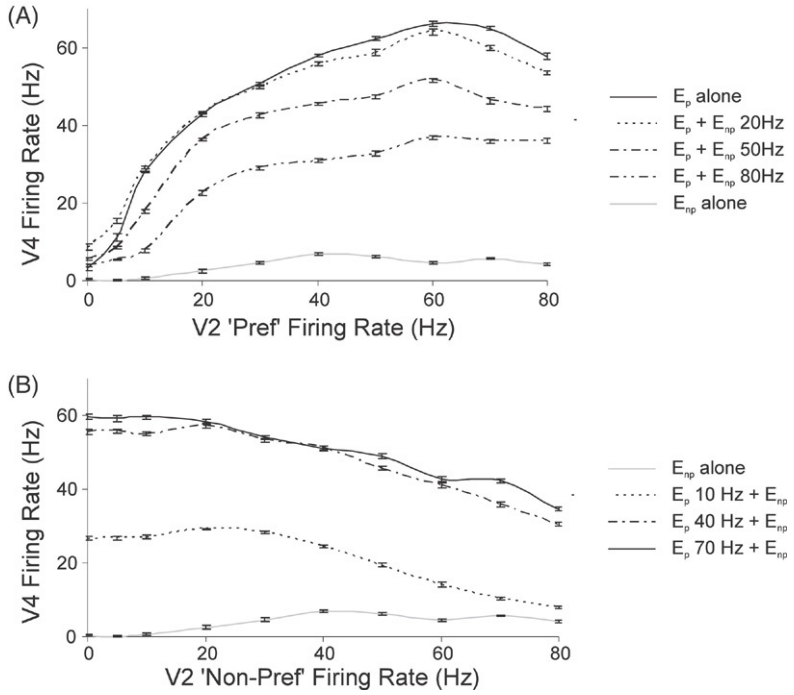

Fig. 6. Average response of the modeled $V4$ neuron as a function of firing rate (contrast) combinations of the preferred and non-preferred synaptic inputs. (A) Average firing rate of the $V4$ neuron during the stimulation period to the preferred stimulus combined with different firing rate (contrasts) inputs from the non-preferred stimulus. Solid black line represents response to preferred stimulus alone i.e. when synaptic input was provided only through the E_p population. The response to the combination of preferred E_p and non-preferred stimulus population E_{np} active at 20 Hz nearly overlaps the response to preferred stimulus alone (dashed line). Response to preferred stimulus input is successively suppressed when combined with the non-preferred stimulus and is most suppressed when non-preferred inputs fire at 80 Hz (double dot dashed line). Response to the non-preferred stimulus input (E_{np}) active alone is shown in light gray. (B) Average firing rate response of the modeled neuron to the non-preferred stimulus input combined with different firing rate (contrasts) inputs from the preferred stimulus. Light gray line represents response to E_{np} active alone. The dashed black line represents the E_{np} activity combined with 10 Hz of preferred stimulus input (E_p) activity. E_{np} combined with more prominent E_p activity of 40 Hz (dot dashed line) or 70 Hz (solid black line). Error bars represent standard error.

of the non-preferred stimulus input, the response of the $V4$ neuron was dominated by the activity of the preferred stimulus population. However, at higher firing rates of the non-preferred input, the neuron's firing rate was not as strongly increased by the presence of the preferred input. This was again due to the large shunting activity of the common inhibitory pool at high firing rates. As can be recalled from Fig. 3(A) the neuron's response to single stimuli saturated at high firing rates due to presynaptic depression dynamics. Hence preferred stimulus input activity at 70 Hz produced an almost equivalent response to input activity at 40 Hz (Fig. 3(A), thick line). This is also reflected in Fig. 6(B) where the combination of the non-preferred stimulus input with the activation of the preferred stimulus input at 70 Hz produced only a slight $V4$ firing rate increase over a response for preferred input combined at 40 Hz. These simulations were similar to the model fits obtained in $V1$ for cross orientation suppression (Carandini et al., 1997).

Together these results suggest that the interplay between feedforward inhibition and synaptic depression may play a critical role in the tuning of $V4$ neurons to preferred and non-preferred stimuli presented alone or together at different contrasts.

3.3. Effect of attention: The role of input correlations

Using simple integrate and fire neuron models, Salinas and Sejnowski (2000, 2002) have shown that correlated spikes from a set of excitatory or inhibitory neurons can in and of themselves result in an increase in the gain of the input–output firing rate curve of the postsynaptic neuron. However, correlations between excitatory and inhibitory inputs cancel out the gain effect. Combinations of correlated excitatory and inhibitory inputs have not been explored in multicompartmental neuron models where perisomatic inhibition may shunt excitatory inputs, and therefore introduce implicit excitatory–inhibitory correlations that might be detrimental to gain increases. In Fig. 7(A) we investigate the effect of correlations only in the excitatory input to the $V4$ neuron. The excitatory input spikes were correlated at a gamma frequency of 40 Hz as has been evidenced *in vivo* in anaesthetized (Castelo-Branco, Neuenschwander, & Singer, 1998; Frien, Eckhorn, Bauer, Woelbern, & Kehr, 1994; Gray & Singer, 1989; Henrie & Shapley, 2005) as well as awake and alert preparations (Gray & Viana Di Prisco, 1997). The spike trains were provided with a 3 ms jitter (Gray, Engel, Konig, & Singer, 1992).

Fig. 7(A) shows an example of the spike input to the neuron from the E_p (left) and I_{ff} (right) pools respectively. In this example 80% of the input synapses from E_p were correlated and no correlations were simulated in the inhibitory pool. The response of the $V4$ neuron to such input is shown below the rastergrams. We simulated three conditions where 30%, 50% and 80% of the excitatory input synapses were

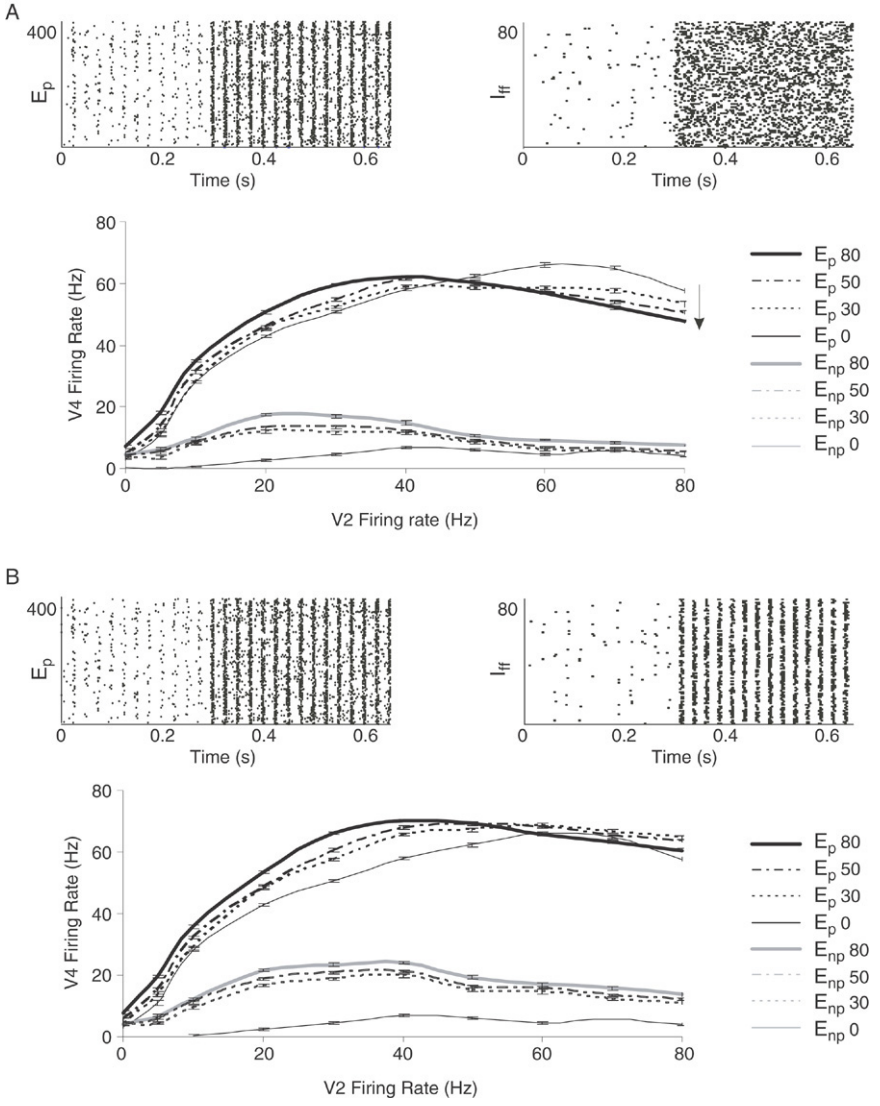

Fig. 7. Modulation of the firing rate of the modeled $V4$ neuron by combinations of correlations in the excitatory and inhibitory input synapses. (A) Top: Rastergrams depicting correlated input spike activity from the preferred (E_p) synaptic population (left) and the non-correlated input spikes from the inhibitory pool (I_{ff}, right). In this examples 80% of excitatory synapses were correlated at a 40 Hz oscillation rhythm. Simulated activity of the $V4$ neuron to such input is shown below the rastergrams. The thin black line depicts the baseline response to the preferred stimulus without any correlation in the synaptic inputs (P 0). Effect of 30%, 50% and 80% preferred excitatory input correlations are represented by the dotted black line (P 30), dot dashed black line (P 50) and thick black line (P 80) respectively. The thin gray line is the baseline response to the non-preferred input without any correlations in the excitatory input (NP 0). Effects of increasing correlation percent to 30%, 50% and 80% are respectively shown by the dotted gray (NP 30), dot dashed gray (NP 50) and thick gray (NP 80) lines respectively. Response increase is seen only at low and intermediate $V2$ input firing rates. Substantial response suppression occurs at high input firing rates only if the excitatory input is correlated (depicted by arrow). In (B) both excitatory and inhibitory synaptic inputs were correlated at 40 Hz oscillation frequency. Correlations in the inhibitory inputs are 12 ms out of phase with respect to the excitatory inputs. The corresponding $V4$ neuron response to such input is shown. All inhibitory inputs were correlated while the % correlation in the excitatory input was changed to 30%, 50% and 80%. Line points are same as those used in panel A. The prominent effect of inhibitory input correlations out of phase with the excitatory input is to remove the response suppression at high firing rates seen when only excitatory input is correlated in the preferred condition.

correlated respectively. The individual preferred and non-preferred excitatory $V2$ inputs were separately correlated. We found that for the preferred excitatory input, correlations boosted the firing rate of the $V4$ neuron above baseline at low and intermediate input firing rates. However, at high input firing rates, correlations in the preferred input actually caused the response of the $V4$ neuron to be depressed (arrow). This happened because the intense random inhibitory spiking at high input firing rates is effectively able to shunt out correlated excitation.

Fig. 7(B) shows an example input to the $V4$ neuron where both excitation and inhibition were correlated. As inhibitory neurons are known to synchronize spontaneously (Fisahn et al., 1998; Wang & Buzsaki, 1996; Whittington, Traub, Faulkner, Jefferys, & Chettiar, 1998) all inhibitory synaptic inputs were correlated. Correlations occurred at spike times defined by the principal gamma frequency of 40 Hz. However, inhibitory input correlations were made to be out of phase with the excitatory input correlations. Support for such a manipulation comes from intracellular $V1$ recordings (Monier et al., 2003) which show

that there exists low temporal overlap between the excitatory and inhibitory inputs to the neuron when it is stimulated by its preferred orientation. The effect of such combined excitatory and inhibitory input correlations is shown. Results in Fig. 7(B) indicate that excitatory correlations coupled with out of phase inhibitory correlations caused an increased firing rate gain effect at low and intermediate firing rates. Within the dynamic response range of the $V4$ neuron between 10 and 40 Hz of input spiking, the firing rate gain effect was of the order of 30% above baseline. This percent change was akin to percent change seen in attention experiments when a $V4$ neuron responded to a preferred stimulus presented in its receptive field (Reynolds et al., 2000).

At higher firing rates, the correlations in inhibitory inputs simulated out of phase with the excitatory input removed the response suppression of the $V4$ neuron seen when only excitatory inputs were correlated (Fig. 7(A) arrow). Thus the combined effect of correlated excitation and out of phase correlated inhibition is to induce a leftward shift in the response threshold of the $V4$ neuron, while maintaining the maximal response at a constant level. Reynolds et al. (2000) have shown that attending to a stimulus resulted in a positive gain of the contrast response threshold of $V4$ neurons. The effect of combined, but out of phase correlations in excitation and inhibition in our multicompartmental neuron with presynaptic short-term facilitation and depression dynamics could simulate and explain such attention modulation to single stimuli.

3.4. Attention modulation of stimulus pairs using input correlations

Selective attention to one of two stimuli in a pair is known to modulate the firing rate response of $V4$ neurons towards the response level of the attended stimulus when it is presented alone. We explore this effect using modulation of input correlations as a biophysical mechanism for attention. For these simulations, both the preferred, E_p and non-preferred, E_pV2 populations were correlated at spike times corresponding to a 40 Hz gamma rhythm. In Fig. 8 correlations were present in 80% of the excitatory synapses. As the two $V2$ input populations represented distinct stimuli their correlated time bins were simulated with distinct phases i.e. the non-preferred $V2$ population had correlations 12 ms out of phase with the correlations in the preferred $V2$ population. This assumption is compatible with results showing that neurons in V1 as well as MT synchronize with other neurons with the same stimulus preference but not with neurons differing in stimulus selectivity (Gray & Singer, 1989; Kreiter & Singer, 1996). In Fig. 7(B) when only one of the two stimuli was active, we simulated the inhibitory pool with correlations out of phase with the correlations of the excitatory synaptic input. Now that both stimuli are active we simulated the correlations in the inhibitory synaptic input at varying phases with respect to the two stimuli. The inhibitory pool was thus simulated at 5 different phase delays ($I_{ff}\mathrm{d}T$) with respect to the correlations in the preferred $V2$ population; 0, 3, 6, 9 and 12 ms. Fig. 8(A) shows an example of correlated input to the $V4$ neuron where inhibition phase ($\mathrm{d}T$) was 6 ms with respect to E_p. For clarity, the non-preferred input E_{np} was always assigned a 12 ms phase delay with respect to E_p. Fig. 8(B) shows the effects of varying phase modulations of the inhibitory input on the spiking of the $V4$ neuron to pairs of stimuli. Inhibitory correlations most out of phase with correlations in the preferred $V2$ input ($I_{ff}\mathrm{d}T = 9$ and 12 ms represented by dotted black and solid black lines respectively) distinctively cause the $V4$ neuron's pair response to shift upwards towards the response to the preferred stimulus presented alone (thick black line). As for $I_{ff}\mathrm{d}T = 0$ ms, when the inhibition is most out of phase with the non-preferred input correlations (dot dashed black line), the neuron's response to the pair was suppressed and resembled the response to the non-preferred input presented alone. Other inhibitory input phase delays of 3 ms and 6 ms (dashed gray and dashed black lines respectively) produced intermediate firing rate modulations. Thus a mechanism that shifts the inhibitory input to $V4$ out of phase with the excitatory input corresponding to the attended stimulus could simulate the effects of selective attention seen in physiological recordings. Further it is interesting to note in Fig. 8(B) that the positive and negative response modulation in the presence of paired stimulus input is prominent at intermediate and high input firing rates but not at low input firing rates. This is compatible with attention experiments where selective attentional bias is prominently observed in spiking responses to high contrast stimulus pairs as opposed to low contrast stimulus pairs (Reynolds & Desimone, 2003).

The time course of the response of the $V4$ neuron to correlated spike input from the preferred and non-preferred stimuli presented individually or in pairs is shown in Fig. 9(A). Stimulus onset was at 300 ms and lasted 350 ms. The four curves from top to bottom are the responses to correlated spiking of the preferred stimulus alone with inhibition out of phase (Attend P), to the preferred and non-preferred stimuli presented together and inhibition out of phase with the preferred stimulus (NP + Attend P), to the two stimuli presented together but inhibition out of phase with the non-preferred stimulus (P + Attend NP), and to the non-preferred stimulus presented alone with out of phase inhibition (Attend NP). These plots resembled the $V4$ neuronal spike responses obtained in selective attention experiments (Reynolds et al., 1999). From these time response plots there was a slight delay when responding to the non-preferred stimulus presented alone, and also when attention is diverted to the non-preferred stimulus in a stimulus pair. This was because the non-preferred spike inputs were provided with a distinct phase delay of 12 ms with respect to the preferred input. To further clarify this point we performed a phase analysis of the four spiking patterns shown in Fig. 9(A) (Fig. 9(B)). The spike phase of the $V4$ neuron was analyzed from 0 to 25 ms as the spike input to the neuron was correlated at a 40 Hz gamma rhythm i.e. in 25 ms bins. In the first phase plot (Attend P), the spikes of the $V4$ neuron were localized within 0–10 ms of phase corresponding to the preferred input presented alone which was phase locked at 0 ms. The second plot (NP + Attend P) shows output spikes when both stimulus inputs were presented but inhibition

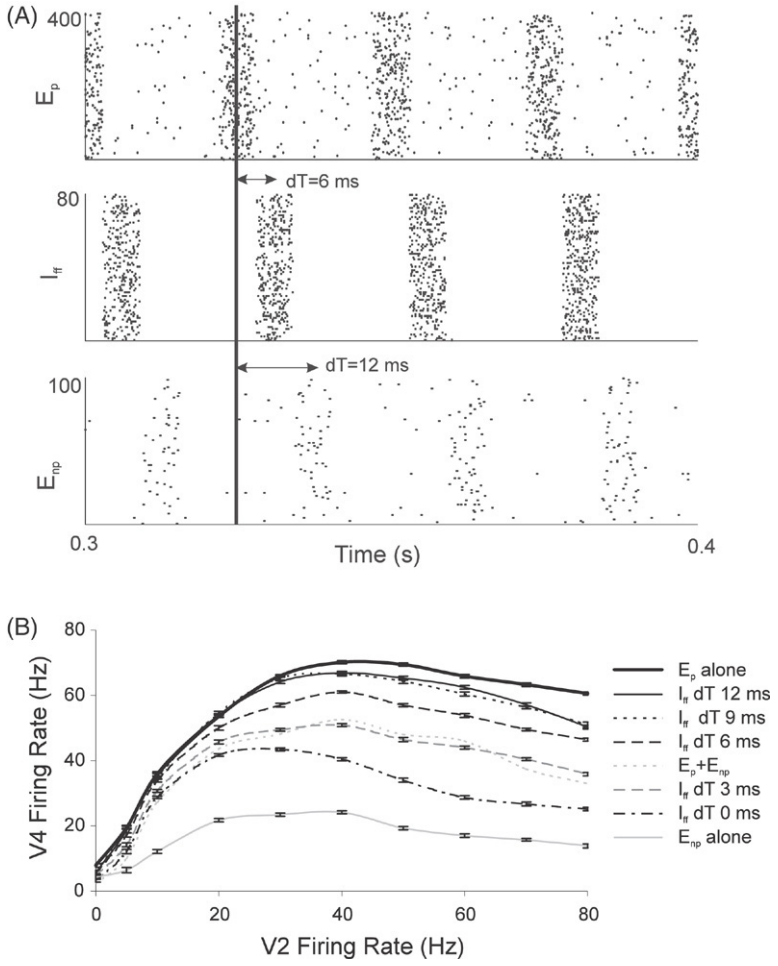

Fig. 8. Response of the modeled neuron to pairs of correlated stimulus input. (A) Rastergrams depicting an example input to the $V4$ neuron. Spike correlations in the preferred synaptic pool (E_p), inhibitory pool (I_{ff}) and non-preferred synaptic pool (E_{np}) are represented from top to bottom respectively. All three input populations have distinct oscillation phase. Phase delays (dT) of I_{ff} and E_{np} with respect to E_p (0 ms phase) are depicted as 6 ms and 12 ms respectively. (B) Response of the $V4$ neuron to distinctly correlated input from E_p, E_{np} and I_{ff}. Reference responses to the preferred stimulus (P) alone (thick black line), non-preferred stimulus (NP) alone (solid gray line) and both stimulus inputs present together without correlated spike activity (P + NP) (gray dotted line) are shown. Correlation phase of E_p and E_{np} were kept constant in all simulations. Shifting the phase of correlations of I_{ff} spikes with respect to correlations in E_p and E_{np} modulates the spiking response of the $V4$ neuron. I_{ff} phase delays (I_{ff}dT) of 12 ms, 9 ms, 6 ms (see also panel A), 3 ms and 0 ms produce response modulations as represented by the solid black, dotted black, dashed black, dashed gray, and dot dashed black lines respectively. Note that significant modulations only occur at firing rates above 20 Hz.

was out of phase with the preferred input or in phase with the non-preferred input. As the non-preferred excitatory spikes were shunted out by correlated inhibition in this case, spiking of the $V4$ neuron again occurred in the 0–10 ms phase bins i.e. the phase response resembled the input spike phase of the preferred input. In the third phase plot (P + Attend NP) spiking of the neuron was distinctly split in the 0–10 ms of phase and 15–25 ms of phase. In this case both correlated preferred and non-preferred input were presented, but inhibition was out of phase with input from E_{np} or in phase with E_p. Hence correlated inhibition shunted out spike inputs from the preferred population and spikes emerged to the non-preferred stimulus input correlated at 12 ms of phase. Finally, when only the non-preferred correlated input was presented (Attend NP) spiking of the $V4$ neuron occurred in the 15–25 ms phase range i.e. closer in phase to the spike phase of 12 ms of the non-preferred input. Thus the phase of the $V4$ neuron's spiking response was also modulated along with its average firing rate by the correlated excitatory and out of phase inhibitory inputs that we simulated.

Fig. 10 plots the average cross correlation across multiple trials for the $V4$ neuron's responses in the four attention conditions. The 40 Hz rhythm was evident in all conditions, especially for attention to preferred stimulus either alone or in presence of a non-preferred stimulus. The firing rate normalized cross correlograms also showed the same trend as the raw correlations, though the gamma frequency modulation for attention to non-preferred stimulus was enhanced by normalization (not shown). Thus cross correlation trends in our model match the firing rate trends. This may not always be the case, such as in simulations of stimulus competition by inhibitory interference by Tiesinga (2005). In their model synchrony precision of inhibitory neurons corresponding to the two stimuli had to be differentially altered apart from the spiking phase modulations to obtain consistent effects across

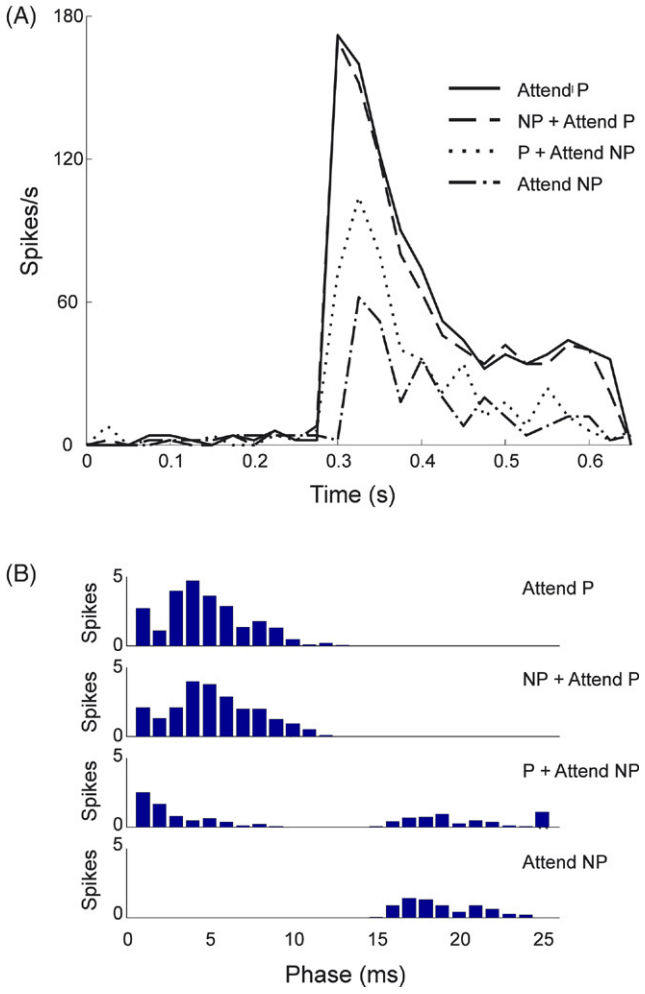

Fig. 9. Spiking of the $V4$ neuron in time to correlated stimulus input. All plots are to excitatory input firing rates of 40 Hz. Preferred input was correlated at the 0 ms phase of oscillation while non-preferred input was correlated at 12 ms phase. Stimulation period is 0.3–0.65 s. (A) The $V4$ neuron's response to correlations in the preferred stimulus presented alone with out-of-phase inhibition (Attend P) is represented by the solid black line. Response to preferred and non-preferred stimulus inputs present together with inhibition out-of-phase with the preferred input correlations (NP + Attend P) is depicted by the dashed line. Both stimuli present together with inhibition out-of-phase with non-preferred input correlations (P + Attend NP) is shown by the dotted line, and the dot-dashed line represents response to non-preferred stimulus presented alone with out-of-phase inhibition (Attend NP). (B) The phase of the four spike responses (shown in panel A) of the $V4$ neuron with respect to the 40 Hz oscillation phase of the input, are respectively plotted from top to bottom. The neuron's response phase resembles the phase of the dominant excitatory input to the neuron that is not shunted by correlated inhibitory spikes from I_{ff}.

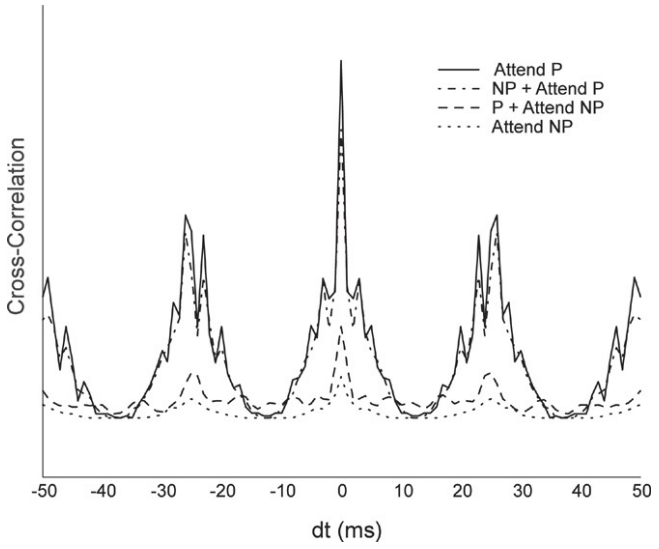

Fig. 10. Cross correlation curves of the spike responses of the $V4$ neuron for the four attention conditions. All plots are to excitatory input firing rates of 40 Hz, and are analyzed for the firing rate curves depicted in 9A. The plots show high correlation peaks corresponding to the 40 Hz gamma rhythm. Responses for attention to preferred stimulus alone (Attend P) or in presence of non-preferred input (NP + Attend P) are depicted by the solid black and dot dashed black lines respectively. Responses for attention to non-preferred stimulus alone (Attend NP) or in presence of preferred input (P + Attend NP) are depicted by the dotted black and dashed black lines respectively.

neuronal firing rates and correlations. Due to the short temporal length (350 ms post-stimulus) of our simulation runs we were unable to construct frequency power spectra for our data, although cross correlations predicted greater 40 Hz power for responses showing attention to preferred than non-preferred stimulus. This is in close agreement with experimental results from intra cranial multielectrode recordings from $V4$ cortex that exhibited greater gamma band power spectral density (PSD) to attended targets compared to attended distracters (Taylor, Mandon, Freiwald, & Kreiter, 2005). The exact experiment simulated in our model comparing gamma band PSD responses of single neurons to attended preferred and non-preferred competing stimuli has not been performed.

We have also explored the robustness of the response modulation achieved for the $V4$ neuron due to correlations in the input spikes. For this we changed both the time jitter of spike correlations as well as the number of correlated synapses (Supplementary data). In all our simulations we used a spike time jitter of 3 ms as has been observed in vivo (Gray et al., 1992). Weaker positive and negative modulation of the paired input response was observed for 1.5 ms and 6 ms spike time jitter. Response modulation was completely abolished at 9 ms of jitter. In vivo experiments in cat $V1$ have shown that neurons efficiently integrated synaptic inputs within a 7 ms time window and spikes separated by a greater time interval were treated as independent (Usrey, Alonso, & Reid, 2000). In our model also, the effect of correlated input with a spike time noise of 9 ms was similar to simulating non-correlated input. In all cases negative response modulation was diminished more than positive response gain, as has also been documented to be the sensitive variable in the stimulus competition by inhibitory interference model (Tiesinga, 2005). Decreasing the number of correlated input synapses from 80% to 50% or 30% significantly diminished response modulation. Thus one limitation of our model is that it requires a large percentage of the presynaptic input to a neuron to be correlated in order for a large range of response modulations to be observed for paired stimulus inputs. This could be due to the absence of any NMDA-receptor mediated synapses in our model that drive recurrent excitation. Incorporation of such synapses has

been shown to amplify the differential activation of competing excitatory populations (Borgers, Epstein, & Kopell, 2005).

3.5. Attention allocation to one of many competing stimuli

We further explored whether the mechanism for attentional modulation proposed here of shifting correlated inhibition out of phase with correlated excitation can also generalize to more than two stimuli. For this purpose spike times from a third excitatory population E_i were added to the model with an intermediate number of 250 synaptic inputs. The corresponding feedforward inhibition was assumed to scale linearly as

$$F_{\mathrm{INH}} = 2\alpha(F_p + F_{np} + F_i)/3. \quad (7)$$

All input populations were correlated with spike times corresponding to a 40 Hz rhythm. The phase relationship of E_p and E_{np} was not changed i.e. they remained 12 ms out of phase as in the simulations above. As E_i represented a moderately preferred stimulus, its correlation phase was modeled 6 ms out of phase with respect to the other two populations, i.e. 6 ms phase delayed with respect to preferred input and 6 ms phase advanced with respect to non-preferred input. To simulate selective attention to one of three stimuli, correlations in the inhibitory pool were shifted out of phase to the attended stimulus, as before. Results are shown in Fig. 11. The $V4$ neuron's firing rate is plotted against $V2$ input in the case where all three excitatory populations were active at the same firing frequency. Spike correlations in the inhibitory pool were simulated at different phase delays, plotted as shown. The neuron's response to the three stimuli was most suppressed for $I_{ff}\mathrm{d}T = 3$ ms (gray line), i.e. for inhibitory correlations that dually interfere with spiking responses to E_p input correlated at 0 ms and also prevent spiking to E_i correlated at 6 ms. For inhibitory phase delays of 0 ms and 6 ms that disrupted spiking to either one of the preferred or the intermediately preferred inputs, larger $V4$ firing rates were observed than for $I_{ff}\mathrm{d}T = 3$ ms (dot dashed black and dotted black lines respectively). All these three phase delays of 0, 3 and 6 ms were farthest in phase from the non-preferred E_{np} input and did not suppress the neuron's firing driven by this population.

The largest firing rate modulations of the $V4$ neuron were observed for $I_{ff}\mathrm{d}T = 12$ ms and 15 ms (dashed bold black and bold black lines respectively) that were most out of phase with the preferred E_p input and disrupted spiking to the non-preferred E_{np} input. Spike phase distributions in Fig. 9(B) indicated that the $V4$ neuron's spike phases spread further out than the exact phase of the impinging synaptic inputs e.g. spike inputs from E_{np} correlated at 12 ms produced spike outputs in the 15–25 ms phase range. Hence, $I_{ff}\mathrm{d}T = 15$ ms which was not in phase but close to E_{np} spiking phase, disrupted the response.

Also, moderately enhanced firing rate gain was observed for $\mathrm{INH}\,\mathrm{d}T = 9$ and 21 ms (dashed black and solid black lines respectively) that were not in phase with the intermediate input population E_i correlated at 6 ms, but optimally positioned to prevent upcoming spiking due to E_p and E_{np} respectively.

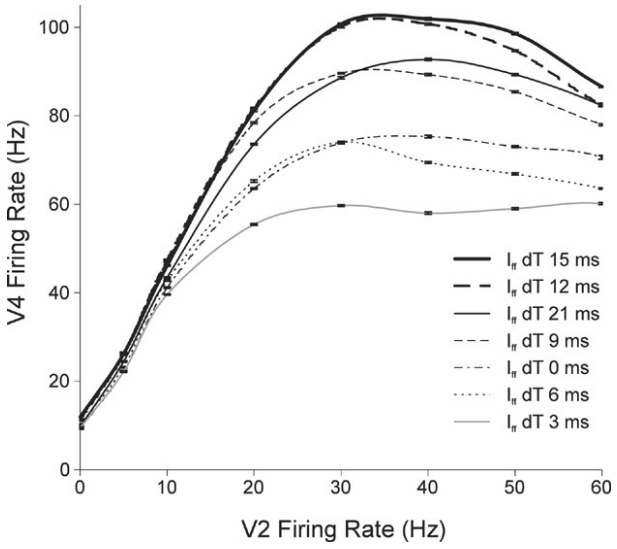

Fig. 11. Firing rate modulation of the $V4$ neuron to three distinctly correlated stimulus inputs. Preferred, moderately preferred and non-preferred excitatory synaptic inputs, E_{np}, E_i and E_{np} were correlated at 0 ms, 6 ms and 12 ms respectively. Shifting the phase of correlations of I_{ff} spikes with respect to correlations in the excitatory populations modulates the spiking response of the $V4$ neuron. I_{ff} phase delays ($I_{ff}\mathrm{d}T$) of 15 ms, 12 ms, 21 ms, 9 ms, 0 ms, 6 ms and 3 ms produce response modulations as represented by the bold black, dashed bold black, solid black, dashed solid black, dot dashed black, dotted black, and gray lines respectively.

Thus, again, a mechanism that allows for feedforward inhibitory phase shifts away from the correlation phase of specific excitation, generates spiking responses that can potentially represent selective attention to one of three presented stimuli. The experimental counterpart to this simulation has not yet been performed.

4. Discussion

4.1. Response to stimulus pairs

In a multi-compartment model of a $V4$ cortical neuron receiving inputs from two $V2$ excitatory synaptic pools and a feedforward inhibitory pool, we have analyzed the neuron's response to combined inputs from both excitatory pools in the absence and presence of presynaptic spike correlations. We generated stimulus preference by modeling a greater number of excitatory synapses from one set of inputs (E_p) than the other (E_{np}). Feedforward inhibition was modeled as broadly tuned with a set of synapses being activated when either the preferred or non-preferred excitatory $V2$ input was active. When both excitatory $V2$ populations were active i.e. when paired stimuli were being presented, the inhibitory input firing rate was increased as a linear function of the firing rates of the individual excitatory inputs. With such input connectivity and with random Poisson spike trains as inputs at every synapse, we were able to generate firing rate responses in the $V4$ neuron to pairs of preferred and non-preferred stimuli that were in between the responses to either stimulus presented alone. In our simulations the $V4$ neuron's response to paired stimuli followed the preferred stimulus for low input firing rates while

at high input firing rates the response resembled an average of the responses to either stimulus presented alone. Physiological experiments that have tested responses to paired stimuli of varying contrast in area MT, the counterpart of area $V4$ in the dorsal visual stream, reported a similar stimulus response relationship. For low contrast stimulus pairs, the response of MT neurons were biased towards the preferred stimulus but robust stimulus averaging occurred at high contrast (Britten & Heuer, 1999; Heuer & Britten, 2002). In our model these effects can be completely accounted for by the simplest assumption of linear inhibition scaling. Thus we show that without any complex spike-time dynamics the underlying excitatory and inhibitory input connectivity to a cortical neuron can itself generate postsynaptic responses to paired stimuli that are approximate weighted averages of responses to individual stimuli.

4.2. Broadly tuned inhibition

Inhibitory interneurons form a heterogeneous class of cells in the cortex. Several studies in cat visual cortex suggest that both inhibition and excitation are well tuned to stimulus orientation (Anderson et al., 2000; Ferster, 1986, 1988). Other experiments especially in primates and ferrets point towards a broader inhibition tuning (Ringach et al., 1997; Roerig & Chen, 2002; Roerig & Kao, 1999). Earlier experiments suggested that inhibitory input in visual cortex may be cross-orientation tuned, i.e. inhibition is best tuned to the non-preferred excitatory stimulus to the neuron (Crook & Eysel, 1992; Crooke, Kisvarday, & Eysel, 1997; Morrone et al., 1982; Pei, Vidyasagar, Volgushev, & Creutsfeldt, 1994). More recent in vivo intracellular recordings in cat visual cortex show that inhibition tuning is heterogenous and variable from cell to cell. While in 60% of the recorded neurons inhibition was tuned to their preferred stimulus, a substantial percentage of neurons had cross-orientation inhibition tuning or even inhibition tuned to other orientations (Monier et al., 2003).

Anatomical data suggest that inhibitory projections in visual cortex are exceeded by excitatory projections in a 1:5 ratio (Anderson et al., 1994; Beaulieu et al., 1992; Fitzpatrick et al., 1987). Hence it seems unlikely that a separate set of inhibitory neurons maybe tuned to each stimulus parameter being represented in cortex. Moreover cortical inhibitory neurons are known to have high firing rates, up to 400–500 Hz (Lacaille & Williams, 1990; McCormick et al., 1985; Wang & Buzsaki, 1996), which could possibly be triggered by multiple stimulus inputs to the same inhibitory pool of neurons. There is also accumulating evidence for extensive gap junction based electrical coupling within inhibitory neurons of the same type (Bartos et al., 2002; Beierlein, Gibson, & Connors, 2000, 2003; Galarreta & Hestrin, 1999, 2001, 2002). However, there is no evidence to suggest that such electrical coupling is functionally driven i.e. that inhibitory neurons are only electrically coupled to other inhibitory neurons with the same functional stimulus preference. Electrical coupling across inhibitory neurons would in fact facilitate broadly tuned inhibition as coupling could spread the activity of inhibitory neurons being driven by a particular stimulus parameter onto other inhibitory neurons that are not strongly driven by that stimulus. Together, these considerations justify our choice for a broadly tuned inhibition (I_{ff}).

4.3. Gamma oscillations

Within mixed excitatory–inhibitory networks two types of mechanisms underlying gamma rhythms have been modeled: Interneuron Network Gamma (ING) and Pyramidal-Interneuron Network Gamma (PING). ING is spontaneously generated in interneuron networks and does not depend on the participation of excitatory neurons, though oscillating interneurons can entrain downstream excitatory neurons to their rhythm. PING on the other hand is modeled in recurrent excitatory–inhibitory networks such that excitatory neurons firing in the gamma range drive and synchronize inhibitory cells and the interneurons in turn gate and synchronize the excitatory population. Excitatory neurons are thus crucial to generating PING. Based on a simplistic PING model Borgers et al. (2005) showed that a combination of modulation of adaptation currents (known to be targets of acetylcholine function in vivo) and differential excitation of two competing excitatory populations can produce excitatory gain for attention to single stimuli, as well as suppress responses of a distractor population in presence of two stimuli. In our study we did not explicitly model excitatory–inhibitory networks that generate gamma rhythms via ING or PING mechanisms. Either architecture is compatible with our assumptions. We instead explored the effects of combined excitatory and inhibitory inputs modeled to have intrinsic gamma frequency contents on a biophysically detailed model of a $V4$ neuron. We presented here a single mechanism based on relative excitatory–inhibitory phase delay that can be invoked to account for attention effects in the visual system of single as well as multiple stimuli.

4.4. The role of correlations in gain modulation

In our multi-compartmental model, we explored the effect of correlated presynaptic activity in both excitatory and inhibitory inputs. The objective of these simulations was to study the responses of $V4$ neurons under different attention conditions (Reynolds & Chelazzi, 2004; Reynolds et al., 1999, 2000; Reynolds & Desimone, 2003). Correlations only in the excitatory input to the neuron synchronized to 40 Hz produced a gain increase in the neuron's response. However, at high input firing rates, excitatory input correlations were strongly shunted by inhibition and produced a decrease in gain. When both excitation and inhibition were correlated but out of phase, the gain increase at low and intermediate firing rates was further enhanced. There was no gain change at high saturating input firing rates. When both $V2$ input stimulus populations were active, correlations in the two excitatory inputs were provided at distinct phases. Correlations from the inhibitory input population could then either be out of phase with input from the preferred $V2$ population or with input from the non-preferred $V2$ population. We were able to increase or decrease

the gain of the $V4$ neuron depending on the phase of the inhibitory input correlations. An increase in the gain of the paired stimulus response was achieved when inhibition was out of phase with the preferred excitatory stimulus population, akin to selective attention to the preferred stimulus. A decrease in gain was achieved when inhibition was out of phase with the non-preferred stimulus population. These gain modulations were essentially accomplished as correlated inhibition was strong enough to shunt out spike input from the non-relevant or non-attended excitatory input. We thus propose a novel mechanism where inhibitory synaptic input correlations out of phase with excitatory input correlations can account for both the sensitivity gain effects of attention to isolated stimuli as well as response gain modulation of selective attention to one of a pair of stimuli. This mechanism works best when the correlation phases of the two excitatory inputs are clearly distinct. This can be thought of as high degree of dissimilarity between the two stimulus inputs, for example for orthogonal stimulus orientations. If however, the two excitatory inputs were to have correlations closer in phase, potentially corresponding to stimuli that are not very distinct from one another, the gain modulation would be much more subtle, as seen in experiments. When a neuron is presented with two stimuli such that its response does not have a clear preference for one or the other stimulus, attention effects are not as strong as when the neuron's response to the two individual stimuli are very different (Reynolds et al., 1999). Taking the model one step further, we also simulated responses of the $V4$ neuron to three competing excitatory inputs with varying phase delays of inputs from the inhibitory pool. The gradient of firing rate modulations obtained in this case can potentially represent selective attention to one of the three differentially preferred visual inputs.

Out of phase excitatory and inhibitory inputs have been observed even at the level of the LGN to V1 projections (Carandini et al., 2002). Intracellular recordings in V1 show that inhibitory and excitatory inputs are anti-correlated for the preferred orientation of the recorded neuron (Monier et al., 2003). Here we propose that when inhibition is dynamically shifted out of phase with the attended stimulus, it is capable of modulating the firing rate gain of $V4$ neurons as seen in attention experiments.

Moreover such a mechanism based on phase modulation of the correlations of the common inhibitory pool can also predict the attention effects on a $V4$ neuron characterized by opposite stimulus preferences to the neuron modeled in these simulations. A neuron with opposite stimulus preference would show opposite positive and negative response gain modulations utilizing the same phase shifts of the correlated spikes of the common inhibitory pool as currently modeled. Thus, such a mechanism can serve as a general mechanism for attentional gain modulation in visual cortex.

When we analyzed the jitter in correlations that is tolerated in the model to generate the response gain modulation effects, we found that up to 6 ms of jitter around the correlated spike bins maintained appreciable positive and negative response modulation of the paired stimulus response. However 9 ms of jitter did not support such modulation as spikes with large correlation jitter are essentially treated as independent spikes. One limitation of the model is that a large proportion of the feedforward synaptic input to the neuron needs to be correlated in order to achieve gain modulation. If 30%–50% of synapses have correlated spikes then the firing response modulation is weak. In these cases, the firing rate modulation of the paired response towards the response to the preferred stimulus presented alone is still achieved, but decreases in responses are more difficult to obtain. This is because preferred stimulus response can only be suppressed if the multitude of synaptic input from the preferred stimulus population appears in a precise time bin to be efficiently shunted by correlated inhibition. Synchronous spiking has in fact been shown to increase with attention in visual (Fries et al., 2001) as well as somatosensory cortices (Steinmetz et al., 2000). Thus a high degree of input correlation is a likely assumption. Though, as mentioned earlier, a lower number of correlated inputs may suffice if NMDA receptor mediated currents were included in the model. Incorporation of such synapses would facilitate recurrent excitation that in turn has been shown to amplify the differential activation of competing excitatory populations (Borgers et al., 2005).

Synchronous spiking has previously been postulated as a mechanism for attentional selection (Niebur, Hsiao, & Johnson, 2002) based on the theoretical work of Crick and Koch (1990). Niebur, Koch, and Rosin (1993) simulated periodic excitatory synchronous V1 inputs onto $V4$ neurons to generate increased $V4$ firing rates. In their model decreased $V4$ firing rates could also be achieved by synchrony based lateral inhibition. However in this model, excitation and inhibition were dedicated to the preferred and non-preferred stimuli respectively. Such specific wiring has not been observed in visual cortex. Moreover mathematical models of synchronous inhibition (Salinas & Sejnowski, 2000, 2002; Tiesinga, 2005) reveal that inhibition synchrony by itself results in an increased rather than decreased gain, as is the case in our model. This occurs because of the post-inhibitory rebound spiking of the post-synaptic neuron. The mechanism suggested here, wherein inhibitory input correlations are dynamically shifted out of phase with respect to the excitatory input correlations corresponding to the attended stimulus can account for firing rate changes seen with attention. Buia and Tiesinga (2006) have recently shown that attentional gain modulation and increased input sensitivity to single stimuli can be modeled in a network of excitatory–inhibitory neurons impinging on an output $V4$ neuron if attention is assumed to correspond to a reduction in driving current to the inhibitory neurons. In their simulations, a delay between the excitatory and inhibitory synchronous volleys emerged during the attention manipulation.

If an excitation–inhibition phase mechanism were viable, how would it be implemented? Recordings from $V4$ neurons combined with microstimulation of frontal eye field (FEF) neurons with overlapping receptive fields result in firing rate modulation effects in $V4$ neurons akin to attentional modulation (Moore & Armstrong, 2003; Moore, Armstrong, & Fallah, 2003). FEF efferents projecting to $V4$ (Stanton, Bruce, & Goldberg, 1995) may mediate the attention effects

by modulating the phase of local inhibitory interneurons. The top-down signal may facilitate the phase delay of the inhibitory input with respect to the feedforward excitatory input from $V2$. Buia and Tiesinga (2006) discuss the possibilities that top-down excitation could drive a separate interneuron population that would in turn inhibit the interneuron pool modeled here. Given the vast diversity of interneuron types this seems plausible. Another possibility could be direct cholinergic mediation wherein acetylcholine may specifically reduce the efficacy of top-down excitation onto the inhibitory pool during attention states. Shifting inhibition out of phase with excitation via modulation from other brain sites is found in hippocampal networks (Toth, Freund, & Miles, 1997). Forebrain septal inputs were shown to selectively inhibit hippocampal interneurons such that hippocampal pyramidal cell discharge and inhibitory cell firing have an out of phase oscillatory rhythm. Information representation and input selection based on oscillation phase is an established mechanism in the hippocampus (Buzsaki & Draguhn, 2004), and is emerging as a computational strategy in many systems (Paulsen & Sejnowski, 2006; Sejnowski & Paulsen, 2006). Whether such a mechanism actually functions in visual cortex requires multilayer recordings in area $V4$, and ideally simultaneously from $V2$ also, from pyramidal neurons as well as inhibitory interneurons. Currently, this is indeed technically challenging. Yet it will be important to analyze the phase of spiking of the recorded neurons to tease apart whether phase shifts in correlated spike activity can indeed account for attention effects.

Acknowledgements

This work was supported by the Howard Hughes Medical Institute, NSF-IGERT grant and National Institute of Health grant # 5R01 MH068481-03.

Appendix. Supplementary data

Supplementary data associated with this article can be found, in the online version, at doi:10.1016/j.neunet.2006.08.005.

References

Ahmed, B., Anderson, J. C., Douglas, R. J., Martin, K. A., & Nelson, J. C. (1994). Polyneuronal innervation of spiny stellate neurons in cat visual cortex. *Journal of Comparative Neurology*, *341*(1), 39–49.

Albrecht, D. G., & Hamilton, D. B. (1982). Striate cortex of monkey and cat: contrast response function. *Journal of Neurophysiology*, *48*(1), 217–237.

Albrecht, D. G., Geisler, W. S., Frazor, R. A., & Crane, A. M. (2002). Visual cortex neurons of monkeys and cats: Temporal dynamics of the contrast response function. *Journal of Neurophysiology*, *88*(1), 888–913.

Anderson, J. C., Douglas, R. J., Martin, K. A., & Nelson, J. C. (1994). Map of the synapses formed with the dendrites of spiny stellate neurons of cat visual cortex. *Journal of Comparative Neurology*, *341*(1), 25–38.

Anderson, J. S., Carandini, M., & Ferster, D. (2000). Orientation tuning of input conductance, excitation, and inhibition in cat primary visual cortex. *Journal of Neurophysiology*, *84*, 909–926.

Archie, K. A., & Mel, B. W. (2000). Dendritic compartmentalization could underlie competition and attentional biasing of simultaneous visual stimuli. *NIPS 2000 proceedings 13*.

Archie, K. A., & Mel, B. W. (2004). Determining the biophysical requirements for dendritic computation of visual stimulus competition and attention modulation. Program no. 175.6. Society for Neuroscience Abstracts.

Bartos, M., Vida, I., Frotscher, M., Meyer, A., Monyer, H., Geiger, J. R., et al. (2002). Fast synaptic inhibition promotes synchronized gamma oscillations in hippocampal interneuron networks. *Proceedings of the National Academy of Sciences*, *99*(20), 13222–13227.

Beaulieu, C., Kisvarday, Z., Somogyi, P., Cynader, M., & Cowey, A. (1992). Quantitative distribution of GABA-immunopositive and -immunonegative neurons and synapses in the monkey striate cortex (area 17). *Cerebral Cortex*, *2*(4), 295–309.

Beierlein, M., Gibson, J. R., & Connors, B. W. (2000). A network of electrically coupled interneurons drives synchronized inhibition in neocortex. *Nature Neuroscience*, *3*(9), 904–910.

Beierlein, M., Gibson, J. R., & Connors, B. W. (2003). Two dynamically distinct inhibitory networks in layer 4 of the neocortex. *Journal of Neurophysiology*, *90*(5), 2987–3000.

Bichot, N. P., Rossi, A. R., & Desimone, R. (2005). Parallel and serial neural mechanisms for visual search in macaque area $V4$. *Science*, *308*, 529–534.

Bonds, A. B. (1989). Role of inhibition in the specification of orientation selectivity of cells in the cat striate cortex. *Visual Neuroscience*, *2*, 41–55.

Borgers, C., Epstein, S., & Kopell, N. J. (2005). Background gamma rhythmicity and attention in cortical local ciruits: A computational study. *Proceedings of the National Academy of Sciences*, *102*, 7002–7007.

Britten, K. H., & Heuer, H. W. (1999). Spatial summation in the receptive fields of MT neurons. *Journal of Neuroscience*, *19*(12), 5074–5084.

Buia, C., & Tiesinga, P. (2006). Attentional modulation of firing rate and synchrony in a model cortical network. *Journal of Computational Neuroscience*, *20*(3), 247–264.

Buzsaki, G., & Chrobak, J. J. (1995). Temporal structure in spatially organized neuronal ensembles: A role for interneuronal networks. *Current Opinion in Neurobiology*, *5*(4), 504–510.

Buzsaki, G., & Draguhn, A. (2004). Neuronal oscillations in cortical networks. *Science*, *304*(5679), 1926–1929.

Carandini, M., Heeger, D. J., & Movshon, J. A. (1997). Linearity and normalization in simple cells of the macaque primary visual cortex. *Journal of Neuroscience*, *17*(21), 8621–8644.

Carandini, M., Heeger, D. J., & Senn, W. (2002). A synaptic explanation of suppression in visual cortex. *Journal of Neuroscience*, *22*(22), 10053–10065.

Castelo-Branco, M., Neuenschwander, S., & Singer, W. (1998). Synchronization of visual responses between the cortex, lateral geniculate nucleus, and retina in the anesthetized cat. *Journal of Neuroscience*, *18*(16), 6395–6410.

Chance, F. S., Abbott, L. F., & Reyes, A. D. (2002). Gain modulation from background synaptic input. *Neuron*, *35*, 773–782.

Crick, F., & Koch, C. (1990). Some reflections on visual awareness. *Cold Spring Harbor Symposia on Quantitative Biology*, *55*, 953–962.

Crook, J. M., & Eysel, U. T. (1992). GABAergic-induced inactivation of functionally characterized sites in cat visual cortex (area 18): Effects on orientation tuning. *Journal of Neuroscience*, *11*, 1347–1358.

Crooke, J. M., Kisvarday, Z. F., & Eysel, U. T. (1997). GABA-induced inactivation of functionally characterized sites in cat striate cortex: Effects on orientation tuning and direction selectivity. *Visual Neuroscience*, *14*, 141–158.

DeAngelis, G. C., Robson, J. G., Ohzawa, I., & Freeman, R. D. (1992). Organization of suppression in receptive fields of neurons in cat visual cortex. *Journal of Neurophysiology*, *68*, 144–163.

Deans, M. R., Gibson, J. R., Sellitto, C., Connors, B. W., & Paul, D. L. (2001). Synchronous activity of inhibitory networks in neocortex requires electrical synapses containing connexin36. *Neuron*, *31*(2), 477–485.

Deco, G., Pollatos, O., & Zihl, J. (2002). The time course of selective visual attention: Theory and experiments. *Vision Research*, *42*(27), 2925–2945.

Desimone, R., & Duncan, J. (1995). Neural mechanisms of selective visual attention. *Annual Review of Neuroscience*, *18*, 193–222.

Dobrunz, L. E., & Stevens, C. F. (1997). Heterogeneity of release probability, facilitation, and depletion at central synapses. *Neuron*, *18*(6), 995–1008.

Dobrunz, L. E., & Stevens, C. F. (1999). Response of hippocampal synapses to natural stimulation patterns. *Neuron*, *22*, 157–166.

Eckhorn, R., Bauer, R., Jordan, W., Brosch, M., Kruse, W., Munk, M., et al. (1988). Coherent oscillations: A mechanism of feature linking in the visual cortex? Multiple electrode and correlation analyses in the cat. *Biological Cybernetics*, *60*(2), 121–130.

Engel, A. K., Roelfsema, P. R., Fries, P., Brecht, M., & Singer, W. (1997). Role of the temporal domain for response selection and perceptual binding. *Cerebral Cortex*, *7*(6), 571–582.

Fellous, J. M., Buntaine, A., Hoang, V., & Bhanpuri, N. (2006). Computational studies of the role of stochastic synaptic transmission in hippocampus and cortex. Program No. 730.11. Society for Neuroscience Abstracts.

Fellous, J. M., Rudolph, M., Destexhe, A., & Sejnowski, T. J. (2003). Synaptic background noise controls the input–output characteristics of single cells in an in vitro model of in vivo activity. *Neuroscience*, *122*, 811–829.

Ferster, D. (1986). Orientation selectivity of synaptic potentials in neurons of cat primary visual cortex. *Journal of Neuroscience*, *6*, 1284–1301.

Ferster, D. (1988). Spatially opponent excitation and inhibition in simple cells of the cat visual cortex. *Journal of Neuroscience*, *8*, 1172–1180.

Fisahn, A., Pike, F. G., Buhl, E. H., & Paulsen, O. (1998). Cholinergic induction of network oscillations at 40 Hz in the hippocampus in vitro. *Nature*, *394*(6689), 186–189.

Fitzpatrick, D., Lund, J. S., Schmechel, D. E., & Towles, A. C. (1987). Distribution of GABAergic neurons and axon terminals in the macaque striate cortex. *Journal of Comparative Neurology*, *264*(1), 73–91.

Frien, A., Eckhorn, R., Bauer, R., Woelbern, T., & Kehr, H. (1994). Stimulus-specific fast oscillations at zero phase between visual areas *V*1 and *V*2 of awake monkey. *Neuroreport*, *5*(17), 2273–2277.

Fries, P., Reynolds, J. H., Rorie, A. E., & Desimone, R. (2001). Modulation of oscillatory neuronal synchronization by selective visual attention. *Science*, *291*(5508), 1506–1507.

Galarreta, M., & Hestrin, S. (1999). A network of fast-spiking cells in the neocortex connected by electrical synapses. *Nature*, *402*(6757), 72–75.

Galarreta, M., & Hestrin, S. (2001). Spike transmission and synchrony detection in networks of GABAergic interneurons. *Science*, *292*(5525), 2295–2299.

Galarreta, M., & Hestrin, S. (2002). Electrical and chemical synapses among parvalbumin fast-spiking GABAergic interneurons in adult mouse neocortex. *Proceedings of the National Academy of Sciences of the United States of America*, *99*(19), 12438–12443.

Gray, C. M., & Singer, W. (1989). Stimulus-specific neuronal oscillations in orientation columns of cat visual cortex. *Proceedings of the National Academy of Sciences of the United States of America*, *86*(5), 1698–1702.

Gray, C. M., Engel, A. K., Konig, P., & Singer, W. (1990). Stimulus-dependent neuronal oscillations in cat visual cortex: Receptive field properties and feature dependence. *European Journal of Neuroscience*, *2*(7), 607–619.

Gray, C. M., Engel, A. K., Konig, P., & Singer, W. (1992). Synchronization of oscillatory neuronal responses in cat striate cortex: Temporal properties. *Visual Neuroscience*, *8*(4), 337–347.

Gray, C. M., & Viana Di Prisco, G. (1997). Stimulus-dependent neuronal oscillations and local synchronization in striate cortex of the alert cat. *Journal of Neuroscience*, *17*, 3239–3253.

Henrie, J. A., & Shapley, R. (2005). LFP power spectra in V1 cortex: The graded effect of stimulus contrast. *Journal of Neurophysiology*, *94*(1), 479–490.

Heuer, H. W., & Britten, K. H. (2002). Contrast dependence of response normalization in area MT of the rhesus macaque. *Journal of Neurophysiology*, *88*(6), 3398–3408.

Hines, M. L., & Carnevale, N. T. (2001). NEURON: A tool for neuroscientists. *Neuroscientist*, *7*(2), 123–135.

Kreiter, A. K., & Singer, W. (1996). Stimulus-dependent synchronization of neuronal responses in the visual cortex of the awake macaque monkey. *Journal of Neuroscience*, *16*(7), 2381–2396.

Lacaille, J. C., & Williams, S. (1990). Membrane properties of interneurons in stratum oriens-alveus of the CA1 region of rat hippocampus in vitro. *Neuroscience*, *36*(1), 349–359.

Luck, S. J., Chelazzi, L., Hillyard, S. A., & Desimone, R. (1997). Neural mechanisms of spatial selective attention in areas *V*1, *V*2, and *V*4 of macaque visual cortex. *Journal of Neurophysiology*, *77*(1), 24–42.

Mainen, Z. F., & Sejnowski, T. J. (1996). Influence of dendritic structure on firing pattern in model neocortical neurons. *Nature*, *382*, 363–366.

Maass, W., & Zador, A. M. (1999). Dynamic stochastic synapses as computational units. *Neural Computation*, *11*(4), 903–917.

McAdams, C. J., & Maunsell, J. H. (1999). Effects of attention on orientation-tuning functions of single neurons in macaque cortical area *V*4. *Journal of Neuroscience*, *19*(1), 431–441.

McCormick, D. A., Connors, B. W., Lighthall, J. W., & Prince, D. A. (1985). Comparative electrophysiology of pyramidal and sparsely spiny stellate neurons of the neocortex. *Journal of Neurophysiology*, *54*(4), 782–806.

Miller, E. K., Gochin, P. M., & Gross, C. G. (1993). Suppression of visual responses of neurons in inferior temporal cortex of the awake macaque by addition of a second stimulus. *Brain Research*, *616*, 25–29.

Monier, C., Chavane, F., Baudot, P., Graham, L. J., & Fregnac, Y. (2003). Orientation and direction selectivity of synaptic inputs in visual cortical neurons: A diversity of combinations produces spike tuning. *Neuron*, *37*, 663–680.

Moore, T., & Armstrong, K. M. (2003). Selective gating of visual signals by microstimulation of frontal cortex. *Nature*, *421*(6921), 370–373.

Moore, T., Armstrong, K. M., & Fallah, M. (2003). Visuomotor origins of covert spatial attention. *Neuron*, *40*(4), 671–683.

Morrone, M. C., Burr, D. C., & Maffei, L. (1982). Functional implications of cross-orientation inhibition of cortical visual cells. *Proceedings of the Royal Society of London*, *216*, 335–354.

Niebur, E., Hsiao, S. S., & Johnson, K. O. (2002). Synchrony: A neuronal mechanism for attentional selection?. *Current Opinion in Neurobiology*, *12*(2), 190–194.

Niebur, E., Koch, C., & Rosin, C. (1993). An oscillation-based model for the neuronal basis of attention. *Vision Research*, *33*(18), 2789–2802.

Qian, N., & Andersen, R. A. (1994). Transparent motion perception as detection of unbalanced motion signals. II. Physiology. *Journal of Neuroscience*, *14*, 7367–7380.

Paulsen, O., & Sejnowski, T. J. (2006). From invertebrate olfaction to human cognition: Emerging computational functions of synchronized oscillatory activity. *Journal of Neuroscience*, *25*, 1661–1662.

Pei, X., Vidyasagar, T. R., Volgushev, M., & Creutsfeldt, O. D. (1994). Receptive field analysis and orientation selectivity of postsynaptic potentials of simple cells in cat visual cortex. *Journal of Neuroscience*, *14*, 7130–7140.

Recanzone, G. H., Wurtz, R. H., & Schwarz, U. (1997). Responses of MT and MST neurons to one and two moving objects in the receptive field. *Journal of Neurophysiology*, *78*, 2904–2915.

Reynolds, J. H., & Chelazzi, L. (2004). Attentional modulation of visual processing. *Annual Review of Neuroscience*, *27*, 611–647.

Reynolds, J. H., Chelazzi, L., & Desimone, R. (1999). Competitive mechanisms subserve attention in macaque areas *V*2 and *V*4. *Journal of Neuroscience*, *19*(5), 1736–1753.

Reynolds, J. H., Pasternak, T., & Desimone, R. (2000). Attention increases sensitivity of *V*4 neurons. *Neuron*, *26*(3), 703–714.

Reynolds, J. H., & Desimone, R. (2003). Interacting roles of attention and visual salience in *V*4. *Neuron*, *37*(5), 853–863.

Ringach, D. L., Hawken, M. J., & Shapley, R. (1997). Dynamics of orientation tuning in macaque primary visual cortex. *Nature*, *387*, 281–284.

Roerig, B., & Chen, B. (2002). Relationships of local inhibitory and excitatory circuits to orientation preference maps in ferret visual cortex. *Cerebral Cortex*, *12*, 187–198.

Roerig, B., & Kao, J. P. Y. (1999). Organization of intracortical circuits in relation to direction preference maps in ferret visual cortex. *Journal of Neuroscience*, *19*, 1–5.

Rolls, E. T., & Tovee, M. J. (1995). The responses of single neurons in the temporal visual cortical areas of the macaque when more than one stimulus is present in the receptive field. *Experimental Brain Research*, *103*, 409–420.

Salinas, E., & Sejnowski, T. J. (2000). Impact of correlated synaptic input on output firing rate and variability in simple neuronal models. *Journal of Neuroscience 15*, *20*(16), 6193–6209.

Salinas, E., & Sejnowski, T. J. (2002). Integrate-and-fire models driven by correlated stochastic input. *Neural Computation*, *14*, 2111–2155.

Sclar, G., & Freeman, R. D. (1982). Orientation selectivity in the cat's striate cortex is invariant with stimulus contrast. *Experimental Brain Research*, *46*(3), 457–461.

Sejnowski, T. J., & Paulsen, O. (2006). Network oscillations: Emerging computational principles. *Journal of Neuroscience*, *26*, 1673–1676.

Singer, W., & Gray, C. M. (1995). Visual feature integration and the temporal correlation hypothesis. *Annual Review of Neuroscience*, *18*, 555–586.

Singer, W. (1999). Neuronal synchrony: A versatile code for the definition of relations? *Neuron*, *24*(1), 49–65, 111–125.

Snowden, R. J., Treue, S., Erickson, R. G., & Andersen, R. A. (1991). The response of area MT and $V1$ neurons to transparent motion. *Journal of Neuroscience*, *11*(9), 2768–2785.

Stanton, G. B., Bruce, C. J., & Goldberg, M. E. (1995). Topography of projections to posterior cortical areas from the macaque frontal eye fields. *Journal of Comparative Neurology*, *353*(2), 291–305.

Steinmetz, P. N., Roy, A., Fitzgerald, P. J., Hsiao, S. S., Johnson, K. O., & Niebur, E. (2000). Attention modulates synchronized neuronal firing in primate somatosensory cortex. *Nature*, *404*, 187–190.

Stevens, C. F., & Wang, Y. (1995). Facilitation and depression at single central synapses. *Neuron*, *14*(4), 795–802.

Stuart, G., & Spruston, N. (1998). Determinants of voltage attenuation in neocortical pyramidal neuron dendrites. *Journal of Neuroscience*, *18*(10), 3501–3510.

Taylor, K., Mandon, S., Freiwald, W. A., & Kreiter, A. K. (2005). Coherent oscillatory activity in monkey area $V4$ predicts successful allocation of attention. *Cerebral Cortex*, *15*(9), 1424–1437.

Tiesinga, P. H. (2005). Stimulus competition by inhibitory interference. *Neural Computation*, *17*, 2421–2453.

Tiesinga, P. H., Fellous, J. M., Salinas, E., Jose, J. V., & Sejnowski, T. J. (2004). Inhibitory synchrony as mechanism for attentional gain modulation. *Journal of Physiology (paris)*, *98*, 296–314.

Toth, K., Freund, T. F., & Miles, R. (1997). Disinhibition of rat hippocampal pyramidal cells by GABAergic afferents from the septum. *Journal of Physiology*, *500*, 463–474.

Usher, M., & Niebur, E. (1996). Modelling the temporal dynamics of IT neurons in visual search: A mechanism for top-down selective attention. *Journal of Cognitive Neuroscience*, *8*(3), 305–321.

Usrey, W. M., Alonso, J. M., & Reid, R. C. (2000). Synaptic interactions between thalamic inputs to simple cells in cat visual cortex. *Journal of Neuroscience*, *20*(14), 5461–5467.

Varela, J. A., Sen, K., Gibson, J., Fost, J., Abbott, L. F., & Nelson, S. B. (1997). A quantitative description of short-term plasticity at excitatory synapses in layer $2/3$ of rat primary visual cortex. *Journal of Neuroscience*, *17*(20), 7926–7940.

Varela, J. A., Sen, S., Turrigiano, G. G., & Nelson, S. B. (1999). Differential depression at excitatory and inhibitory synapses in visual cortex. *Journal of Neuroscience*, *19*(11), 4293–4304.

Wang, X. J., & Buzsaki, G. (1996). Gamma oscillation by synaptic inhibition in a hippocampal interneuronal network model. *Journal of Neuroscience*, *16*(20), 6402–6413.

Wang, H. -P., Fellous, J. M., Spencer, D., & Sejnowski, T. J. (2005). Supralinear reliability of cortical spiking from synchronous thalamic input (in peparation).

Whittington, M. A., Traub, R. D., Faulkner, H. J., Jefferys, J. G., & Chettiar, K. (1998). Morphine disrupts long-range synchrony of gamma oscillations in hippocampal slices. *Proceedings of the National Academy of Sciences of the United States of America*, *95*(109), 5807–5811.